Analytical Methods for Tracking Body Movements on the Lunar Surface in Apollo XVI Footage

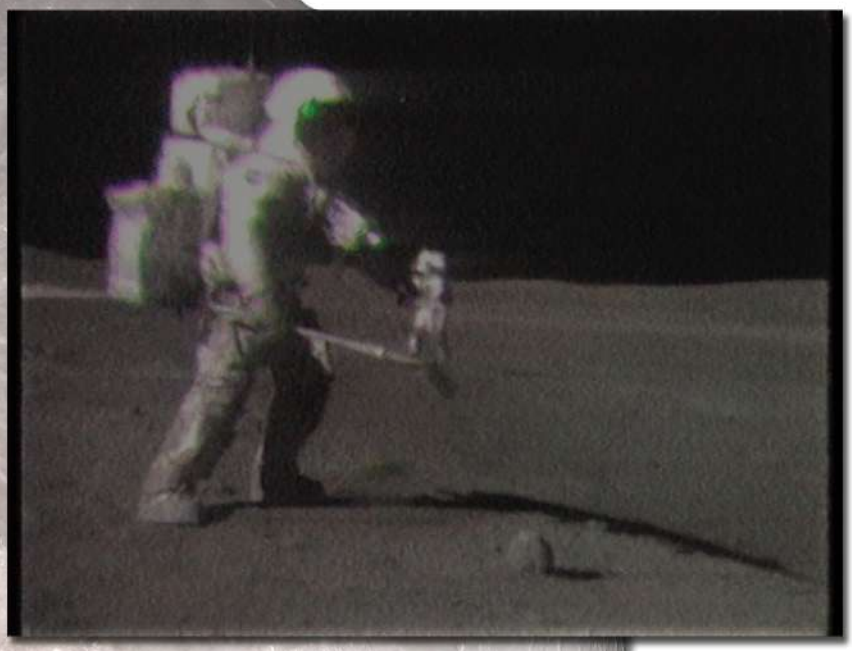

https://doi.org/10.32388/IA8MXE.2

ACKNOWLEDGMENTS

Many people, directly and indirectly, have made this study possible through their collaboration. Most of them have not had the opportunity to see the full content of this work, which may be partly outside their respective research fields. Furthermore, the final results of this paper may not reflect, or be in contradiction with, their beliefs or research. However, we would like to thank each of them for their help and for the effectiveness of their valuable contribution.

We would like to thank for their methodological suggestions and encouragement in research: prof. Luis Bilbao, Universidad de Buenos Aires - Departamento de Física; prof. Andrea Simon, Scuola Superiore Novalis, San Vendemiano (Treviso, Italy); prof. Pasquale Bosso, University of Lethbridge (Canada); prof. Derek Bolton, University of Oxford (United Kingdom); Prof. Franco Macchini, University of Pisa (Italy).

This paper would not have been possible without the technical information, scientific support and documentary materials provided by:

- James T. Hawes, IT Expert technical, writer & editor
- Mark Gray, Spacecraft Films (Atlanta GA), NASA contractor for Video Editing
- Russ Andersson, SynthEyes, Andersson Technologies LLC (Phoenixville, PA)
- Douglas Brown, Open Source Physics (OSP), Davidson College, Davidson NC, USA

The first version of this paper has already been reviewed by the following researchers:

- **Andreas Märki**, Zurich (CH); Master of Engineering, Swiss Aerospace Industry Technician. Revised sections: Preamble; Sections A, B, C, D.

- **Luis Bilbao**, Buenos Aires (ARG); PhD at the Physics University of Buenos Aires; more than 100 publications in international journals; reviewer for the American Journal of Physics and other major scientific journals. Revised sections: Sections B, E.

- **Dwight Steven-Boniecki**, Köln (DE); Author of Space History: NASA Skylab and Soyuz Mission Reports Editor/Compiler. Revised sections: Preamble; Section A.

- David Chandler, Denver, Colorado (USA); Teacher at Porterville College, Porterville, CA / Physics, Mathematics, and Engineering; publications in American Journal of Physics and other Journals. Served on “The Physics Teacher” Editorial Board as a reviewer.
Revised sections: Preamble.

- **Francesco Vinci**, Avola (IT); Order of Architects P.P.C. Siracusa province; Teacher at Università degli Studi di Catania, Facoltà di Scienze dell’Architettura e dell’Ingegneria Edile. Creator of “Brunelleschi” software for prospective restitution. Revised sections: Preamble; Section A.

Their contribution to the review process is documented in a specific appendix (not attached here).

English translation by Roberto Leopardi

ABSTRACT

This manuscript introduces a robust analytical method to trace and analyze the movement of bodies shooting past the Apollo XVI mission on the lunar surface. By employing both 2D and 3D analysis techniques, we aim to provide a detailed comparison of the observed kinematic events against theoretical models.

The paper extends a previous work focused on the kinematics of lunar dust utilizing footage from the "Grand Prix" sequence of the Apollo XVI mission ("Ballistic motion of dust particles in the Lunar Roving Vehicle dust trails" published in 2012 on the American Journal of Physics by Mihaly Horanyi and Hsiang-Wen Hsu: https://www.researchgate.net/publication/258468670 [*Ann. 1* – *Ann. 2*].

The objective is to validate lunar environmental models and enhance the understanding of motion dynamics on the lunar surface. This comprehensive analysis reconstructs the image production chain and the photographic and television transmission technology used during the Apollo 16 mission and indicates the good practices to follow for the correct digital transposition of the various types of film produced. Not only does it reassess existing data but also introduces new methodologies in order to interpret the lunar surface motions of bodies captured during Apollo missions.

THE AUTHORS

Alessio Michelotti
was born in Lucca (IT) the 31-08-72, and obtained a scientific high school diploma at the Liceo Lorenzini in Pescia in 1991 with a specialization in Physics - Mathematics. He is a professional researcher in the field of Culture with different publications edited by academic publishers in Italy (like Bulzoni Editore and CUEM).
Orcid: 0000-0002-3822-104X

PhD Andrea Simon
Headmaster in the "Novalis" Italian Waldorf High School where he is also a mathematics and physics teacher, he obtained his Master's Degree in Physics and his teaching qualification from the University of Padua. Among the most significant previous published works, is "*First Results of a Scintillating GEM Detector for 2-D Dosimetry in an Alpha Beam*" edited by IEEE in 2008.
Orcid: 0009-0001-3971-4305

PREAMBLE
The study of Horanyi-Hsu, approach, and criticalities

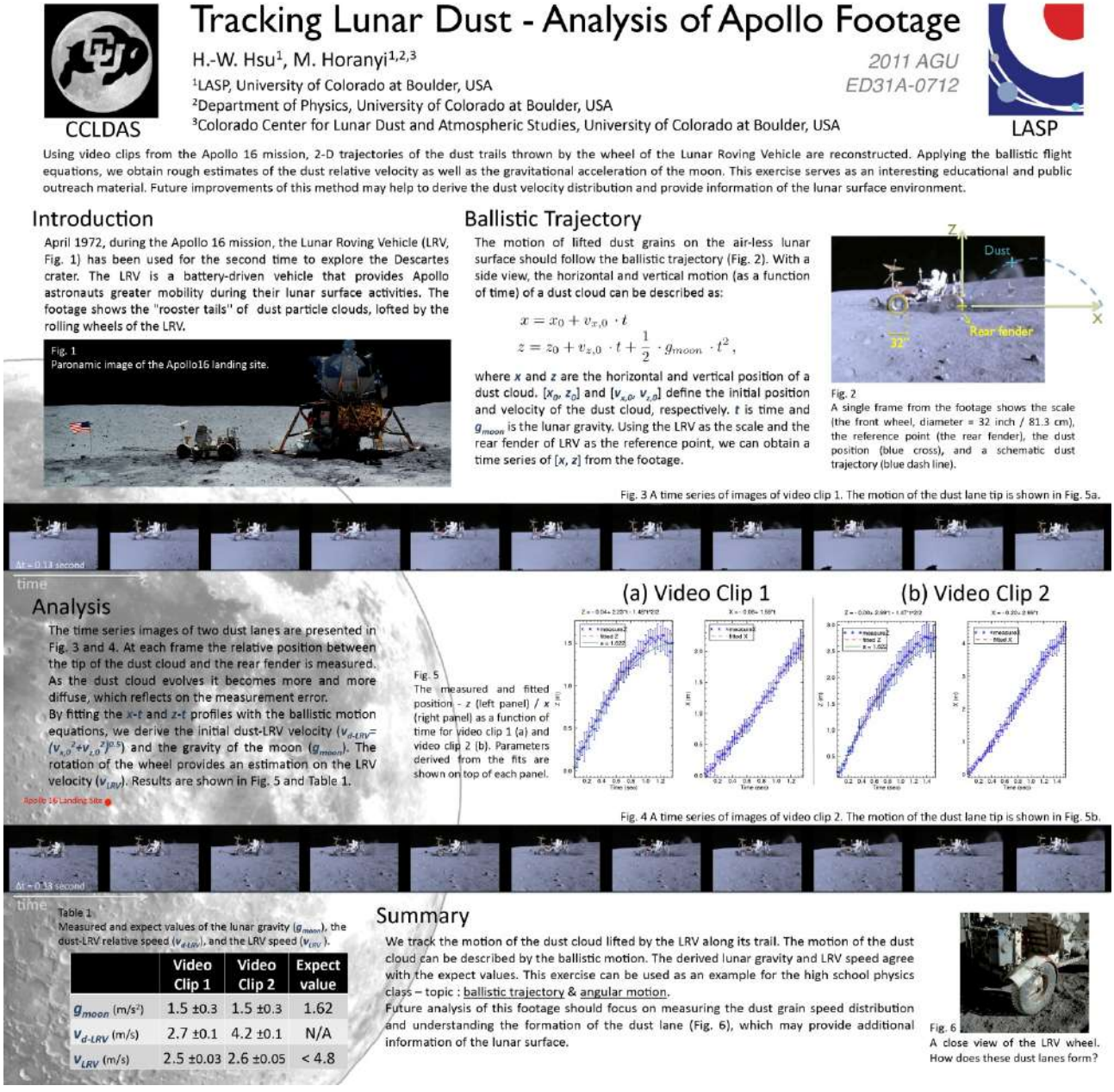

Figure 1- "Tracking Lunar Dust" – Poster by Hsiang-Wen Hsu

Mihály Horányi and Hsiang-Wen Hsu of the Laboratory of Atmospheric and Space Physics (University of Colorado Boulder, NASA Lunar Science Institute) carried out the study "**Ballistic motion of dust particles in the Lunar Roving Vehicle dust trails**" in 2011, with the stated intent to suggest a useful educational path on ballistic trajectories and angular motion for high schools and introductory university physics courses. Following its publication in the American Journal of Physics, in May 2012, the study benefited from important attention, also through the media, in the context of the debate on the authenticity of the Apollo missions, given the results achieved in

identifying the characteristics of the motion of the lunar dust triggered by the Lunar Rover in the famous Apollo 16 sequence known as the "Grand Prix".
Unfortunately, the study presents a series of shortcomings and critical issues that invalidate its scientific results. Far from wanting to go into the merits of the debate on the authenticity of the lunar missions, before starting the discussion of this study, we intend to summarize the problems that the paper of the two researchers of the American team presents.

Errors in basic technical assumptions.

In the introduction, the study in question proposes the recordings of the Apollo TV camera as the source of the analyzed images, asserting that this camera was able to provide "*high resolution color video that was transmitted in real-time to Earth*". Paragraph II of the script then begins by affirming that "*the frame rate of the TV camera used during the Apollo 16 mission was 29.97 fps*", supported by note 2 which refers to the "*Apollo color television subsystem: Operation and training manual*" of the Westinghouse Defense and Space Center, 1971. Immediately after the authors continue: "*The footage was digitally scanned and transformed into a series of images*".

Indeed, as verifiable in the Apollo 16 Index of Photographs and Film Strips [1], drafted by NASA (Manned Spacecraft Center Houston, Texas) in 1972, the sequence named "Grand Prix" was filmed by the Maurer Data Acquisition Camera (DAC) at 24 fps.

Figure 2 - Maurer Data Acquisition Camera (DAC)

[1] https://www.hq.nasa.gov/wp-content/uploads/static/history/alsj/a16/a16.photidx.pdf *Apollo 16 index of 70 mm Photographs and 16 mm filmstrips pag 19, Manned Spacecraft Center Houston, Texas - November 1972* [Ann. 3]

Furthermore, the camera used in the EVA (Extra Vehicular Activities) of the Apollo 16 mission was not the Westinghouse, but the RCA's Colour TV (CTV). The latter, among other things, was unable to send to the Earth high-definition images of a quality comparable to those recorded by the DAC. On the contrary, the television images had very low quality due to a series of problems related to the availability of bandwidth for sending the signal and to the necessity of converting the images into the NTSC standard of the television circuit (29,97 interlaced fps).

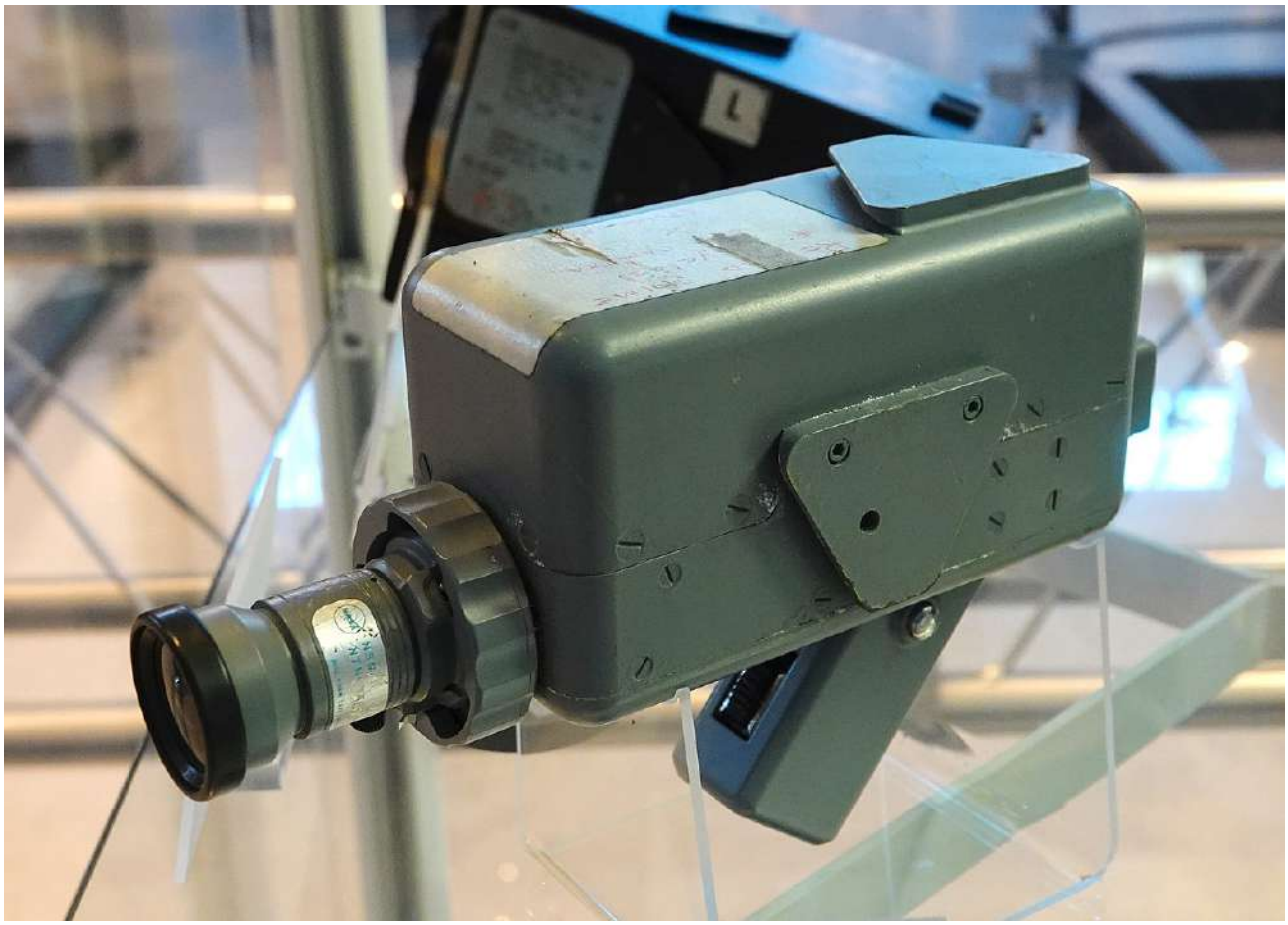

Figure 3 - RCA CTV Camera, at Steven F. Udvar-Hazy Center Virginia US

By verifying the sources that the authors of the study have released, it is clear that the analysed frames contain one clone for every 4 images. This is evident by scrolling the images in succession [2]. This is a typical phenomenon called 3:2 pulldown, through which are carried out the conversions from 24 fps format to 30 fps television format.

The images analysed by Horanyi-Hsu do not represent the digitization of the original film, as stated in the study, but indeed the copy of subsequent NTSC television versions for which, among other things, the number of suffered conversions and alterations is not known.

It is surprising to find that who made the measurements on the images has identified a movement of the lunar dust even on the cloned frames. Not only this is obviously impossible, but it also makes the entire measurement procedure used hardly credible.

[2] https://youtu.be/MI4_H7rqkG8 *"Grand Prix sequence" / Clip2, Apollo 16 – Video a 1 fps x 46 frames* [Ann. 4]

Here below is an extract from one of the two tables of measurements released by the team of the American university, relating to the first analysed clip. Measurements are in pixels. The scale is of 0,0148 m/pixel.

Image number	X_fender	Z_fender	X_dust	Z_dust
4192	422	235	476	165
4193	420	235	476	162
4194	416	236	476	157
4195	411	231	476	152
4196	403	232	476	150
4197	402	232	476	150
4198	398	235	478	148
4199	393	236	478	147
4200	392	235	478	144
4201	392	234	483	140
4202	392	234	483	141 ±2
4203	390	232	485	136 ±2
4204	387	231	488	130
4205	387	230	497	127
4206	389	228	501	122
4207	388	228 ±1	503 ±3	123
4208	392	223 ±3	512 ±4	120
4209	396	223	518	116

Table 1 – Extract from table Clip 2 of "Tracking Lunar Dust" study of Horanyi-Hsu

The lines marked in yellow refer to the frames cloned from those immediately preceding due to the conversion process. As you can see in the red boxes, the values collected by the authors highlight differences between the original frame and the cloned frame which in some cases even reach 5 pixels (equivalent in reality to about 7.5 cm) and in one case 9 pixels (over 13 cm in the reality). Whereas in some cases the error remains within the confidence interval, admitting considering as such the sum of the absolute errors declared for the measurements of each of the two identical frames, in other cases it exceeds it of 1 or 2 pixels, thus proving that the confidence interval is too optimistic.

Regardless of the correctness of the measurement system, the use of an incorrect frame rate has - as it will be easily understood - an important impact on the analysis of the speed of the dust, considering that between one event and another does not elapse 1/29.97 seconds as supposed by authors, but 1/24 seconds infact.

Also, in chapter II of the study to which we refer, it is asserted that *"The resolution of the images is 720x480 pixels"*. This statement leads us to suppose that a correct conversion of images filmed with analogical technology into digital homographic images has not been made. The DAC camera in fact had a 16 mm sensor and therefore produced images with an aspect ratio of 10,26 mm / 7,49 mm =

1,37 while the aspect ratio relating to the indicated resolution is 1,5. This does not necessarily lead to a change in aspect ratio since the different aspect ratios of the converted image could be related to a cropping of the original one.

The presence of black side bands (Nominal Analogue Blanking) in the photographic sources released, indicates that the analysed images come from a television video, presumably a conversion to the NTSC TV format at 29.97 fps of the original sequence filmed at 24 fps. The real aspect ratio of the images themselves, considering the black columns of 8 pixels on each side, is therefore 704 x 480 rectangular pixels. In order to be correctly displayed on the PC while maintaining the same aspect ratio, the frames in question would have required an adjustment of the proportions by a reduction of 10/11 of their width, as required by the good practices defined by the international standards [3]. If the aspect proportion had been respected, by measuring horizontally and vertically the diameter of the Rover wheels on the images that the study authors provided, an identical measurement should have been found. After performing various tests on different frames, it is found that the ratio between the vertical axis and the horizontal axis is equivalent to about 9,1 (10/11). This confirms the missed adjustment.

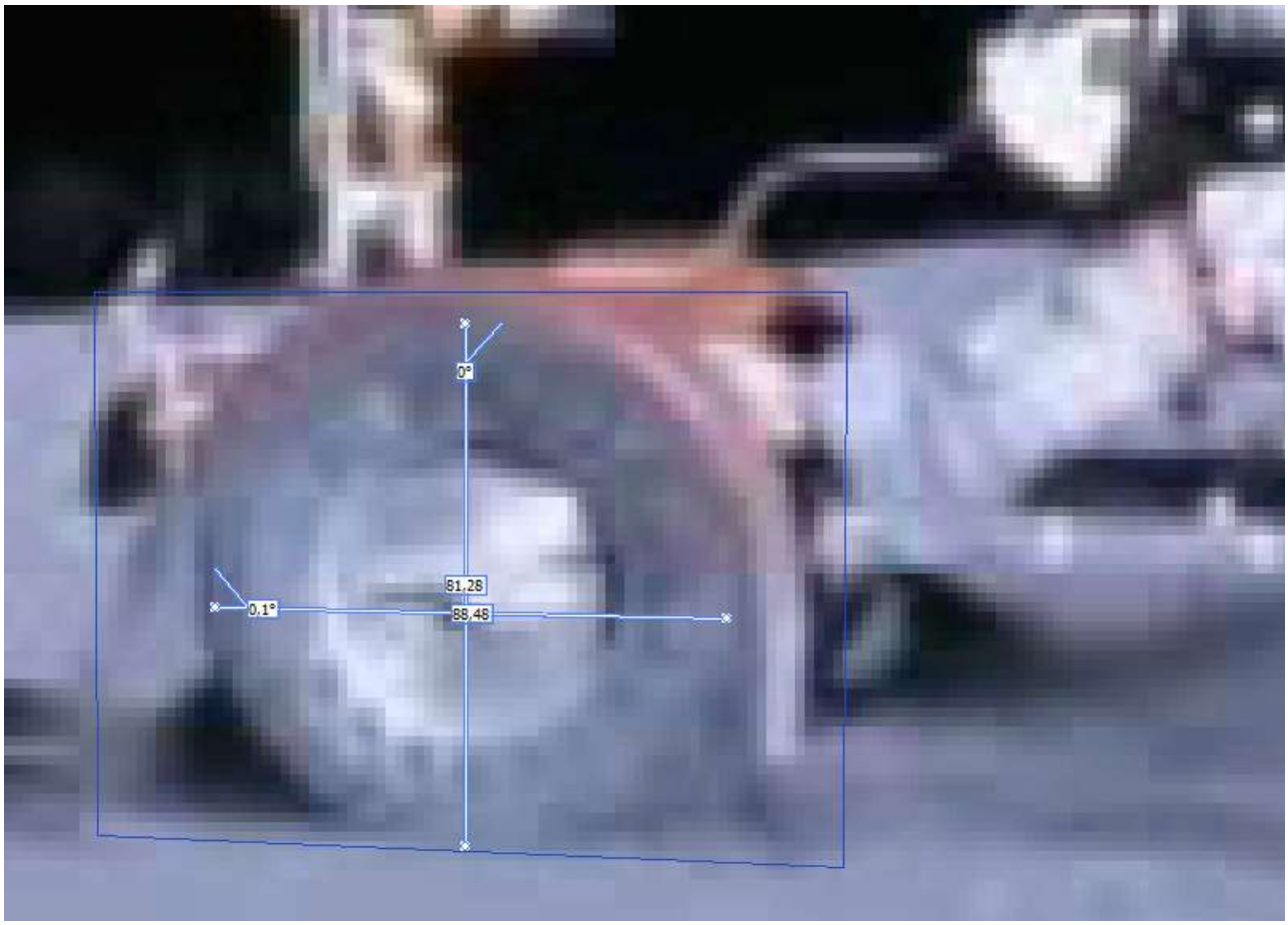

Figure 4 – Verification of the correct aspect ratio of the images analysed by Horányi and Hsu

[3] *https://www.itu.int/dms_pubrec/itu-r/rec/bt/R-REC-BT.601-7-201103-I!!PDF-E.pdf: Studio encoding parameters of digital television for standard 4:3 and wide screen 16:9 aspect ratios, Recommendation ITU-R BT.601-7 (03/2011). International Telecommunication Union Electronic Publication, Radiocommunication Sector, Geneva 2017* [*Ann. 5*]

Lunar Rover wheel: Vertical Axis / Horizontal Axis = cm 81,28 / cm 88,48 = 0,919

Due to this lack of conversion, the images are distorted on the X axis of the measurement system used, and the measurements collected on this axis are therefore burdened by an incorrect increase of 11/10 compared to the measurements detected on the Z axis. Since the calibration of the system scale was carried out starting from a known measurement identified on the X axis (the radius of the Rover wheel), it follows that the values measured on Z are 1/10 lower than the correct ones.

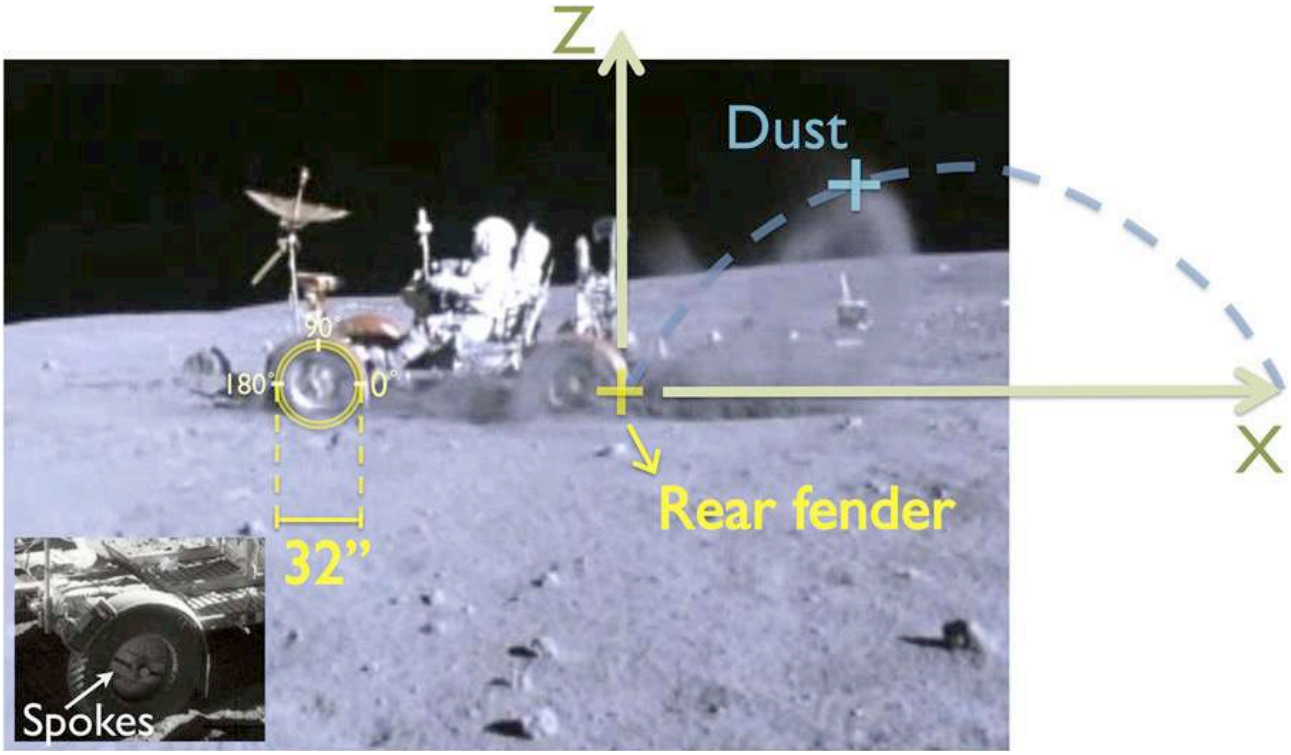

Figure 5 - "Tracking Lunar Dust" of Horanyi-Hsu, calibration of the measuring system

In this regard, we also note that the same measurement of the Rover wheel diameter is proposed as 32 inches, while NASA's Apollo Lunar Roving Vehicle manual identifies it as 32.2 inches. [4]

Image Distortion Analysis

The two authors of the study do not in any way deal with the problems related to the geometric distortion of the analysed images that could derive from the optics used for shooting. The conclusions on this topic can be drawn by means of elementary calculations, starting from the knowledge of the characteristics of the equipment used. These are conclusions that incidentally confirm that the problem can be overlooked, but the absence of any treatment in Horanyi and Hsu's study is far from justified.

[4] https://www.nasa.gov/wp-content/uploads/static/history/alsj/LRV_OpsNAS8-25145.pdf *Lunar Roving Vehicle Operation Handbook, The Boeing Company LRV Systems Engineering, Huntsville (Alabama, USA) April 19, 1971* [*Ann. 6*]

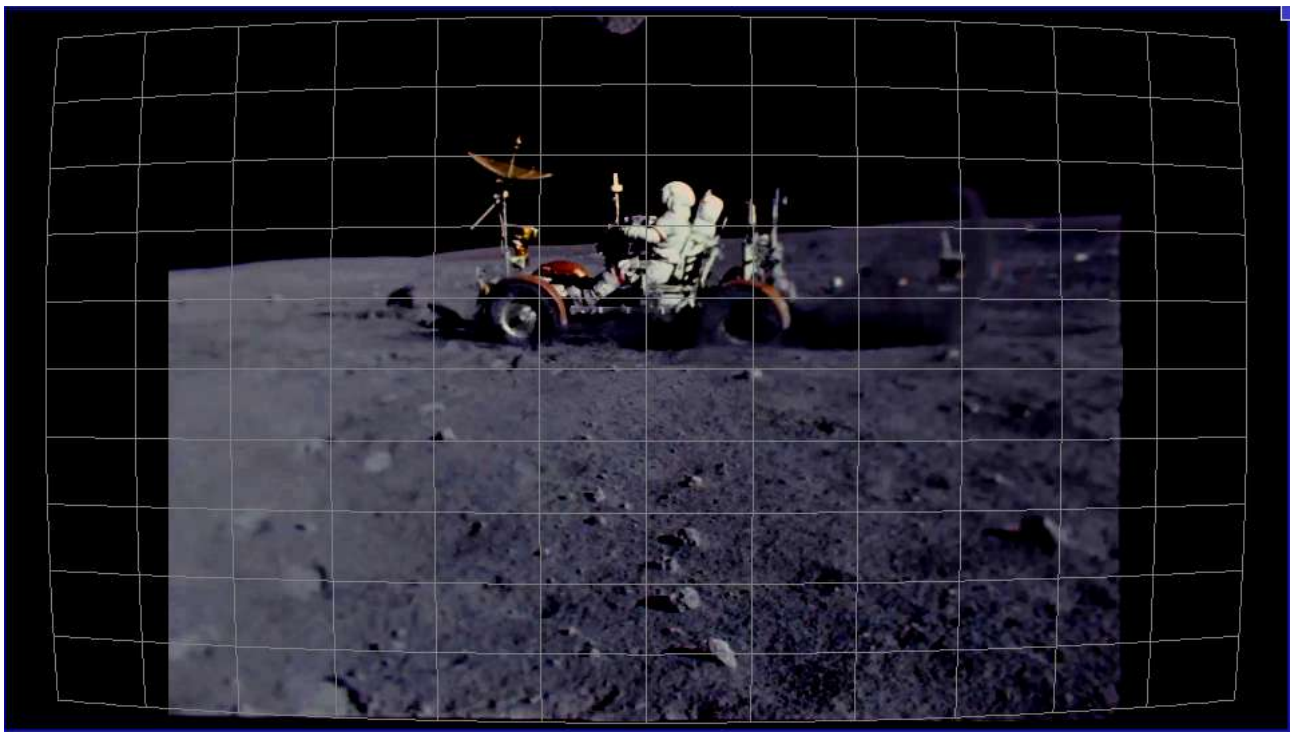

Figure 6 – Barrel distortion simulation for the "Grand Prix" sequence taken with the DAC by C. Duke

The Grand Prix sequence was actually shot with a 10mm SWITAR wide-angle lens [5], manufactured by Kern & Co. of Aarau (Switzerland) [6]. By knowing the dimensions of the 16 mm sensor of the machine, it is possible to calculate the equivalent focal length (F_e) to the standard format (35 mm), a value that can give an indication of the percentage of geometric distortion to be applied.

Focal Length used: F = 10 mm
Dimensions of Maurer DAC sensor: 10,26 x 7,49 mm (16 mm format)
Diagonal of sensor: D = $\sqrt{(10{,}26^2 + 7{,}49^2)}$ = 12,70 mm
Diagonal of 35 mm format: D_s = 43,3 mm

$$F_e = \frac{F \times Ds}{D} = \frac{10 \times 43{,}3}{12{,}70} = 34{,}10 \text{ mm}$$

Lenses with a fixed focal length could result in minimal distortion phenomena of the "barrel" type, with a percentage error starting from 0% for 70-35 mm focal lengths and ending to 1% for the shorter ones. Considering that we are very close to the threshold value and that the technical information available on the lens used testifies its excellent performance in low distortion, we can consider as negligible its geometric aberration.

---

[5] *https://www.hq.nasa.gov/wp-content/uploads/static/history/alsj/JSC-07210PltOpsEquip.pdf Handbook of Pilot Operational Equipment for Manned Space Flight. Report No. CD42-A/SL-997. Prepared By. POE Development Section, NASA, Lyndon B. Johnson Space Center, Houston, Texas; June 1973* [Ann. 7]

[6] *https://www.kern-aarau.ch/fileadmin/user_upload/Aldo/Optik/Haefliger_Kameras_Optik_Objektive_NASA.pdf Kern Objektive für das Apollo Raumfahrtprogramm der NASA, von Rolf Häflinger, Photographica Cabinett 67/2016* [Ann. 8]

Lack of an analysis system

In paragraph II of the study, the NASA Lunar Science Institute team states the following: "*For our analysis, we chose periods of time when the velocity vector of the LRV is approximately constant and orthogonal to the camera line of sight. This choice simplifies the analysis to a two-dimensional geometry*".

It is easy to imagine the limits of the hypothesis of a constant motion of the LRV, given the extreme roughness of the lunar soil and the time intervals involved (in the order of 1/24 second): this makes conceptually weak the method of determining the initial speed of the column of dust that the Colorado scholars propose to adopt and which, as already mentioned, is based on the angular speed of the vehicle wheel. This weakness later proves to be effective also experimentally.

In fact, the measurements performed by the team on the rotation angle of the spokes that depart from the centre of the wheel, confirm a significant fluctuation, with intervals that for example in clip 2 range from $\Delta\Theta = 4$ deg. to $\Delta\Theta = 37$ deg.

$T = 1/24$ s; $\Omega = (\Theta_1 - \Theta_0) / T$; $V_{LRV} = R\Omega$;
Wheel circumference of LRV = 2,57 m

Image number	Θ (deg.)	Δ Θ (deg.)	T (s)	Ω (m/s)	V_{LRV} (m/s)
2148	306	4	0,042	0,68	0,29
2149	302				
...	...	...			
2152	357	27	0,042	4,59	1,88
2153	24				
...	...	...			
2159	88	7	0,042	1,19	0,49
2160	95				
...	...	...			
2169	222	37	0,042	6,28	2,57
2170	259				
...	...	...			
2177	319	16	0,042	2,72	1,11
2178	335				

Table 2 - *Extract from table of "Tracking Lunar Dust" by Horanyi-Hsu, Clip 2: Θ intervals and resulting LRV speed*

Assuming a constant speed, these fluctuations in the unit of time should remain within the proposed confidence interval which in this clip is $\Delta V_{LRV} = \pm 0{,}05$ m/s. But, as can be seen from table 2, they even go as far as to obscure the declared Rover Speed data: $V_{LRV} = 2{,}6$ m/s.

The second part of the just mentioned statement (*"the speed vector of the LRV is orthogonal to the plane of view of the camera")* deserves a check. A chance to verify this claim in relation to Clip 2 is

given by the work conducted by Russ Andersson, founder of Andersson Technologies LLC and developer of SynthEyes, one of the most accredited 3D camera tracking software.

Precisely on this very famous sequence, Andersson performed a 3D analysis tracing the movement of objects and the camera for 173 frames, then released the sources of the analysis as a demonstration example for the software users. [7]

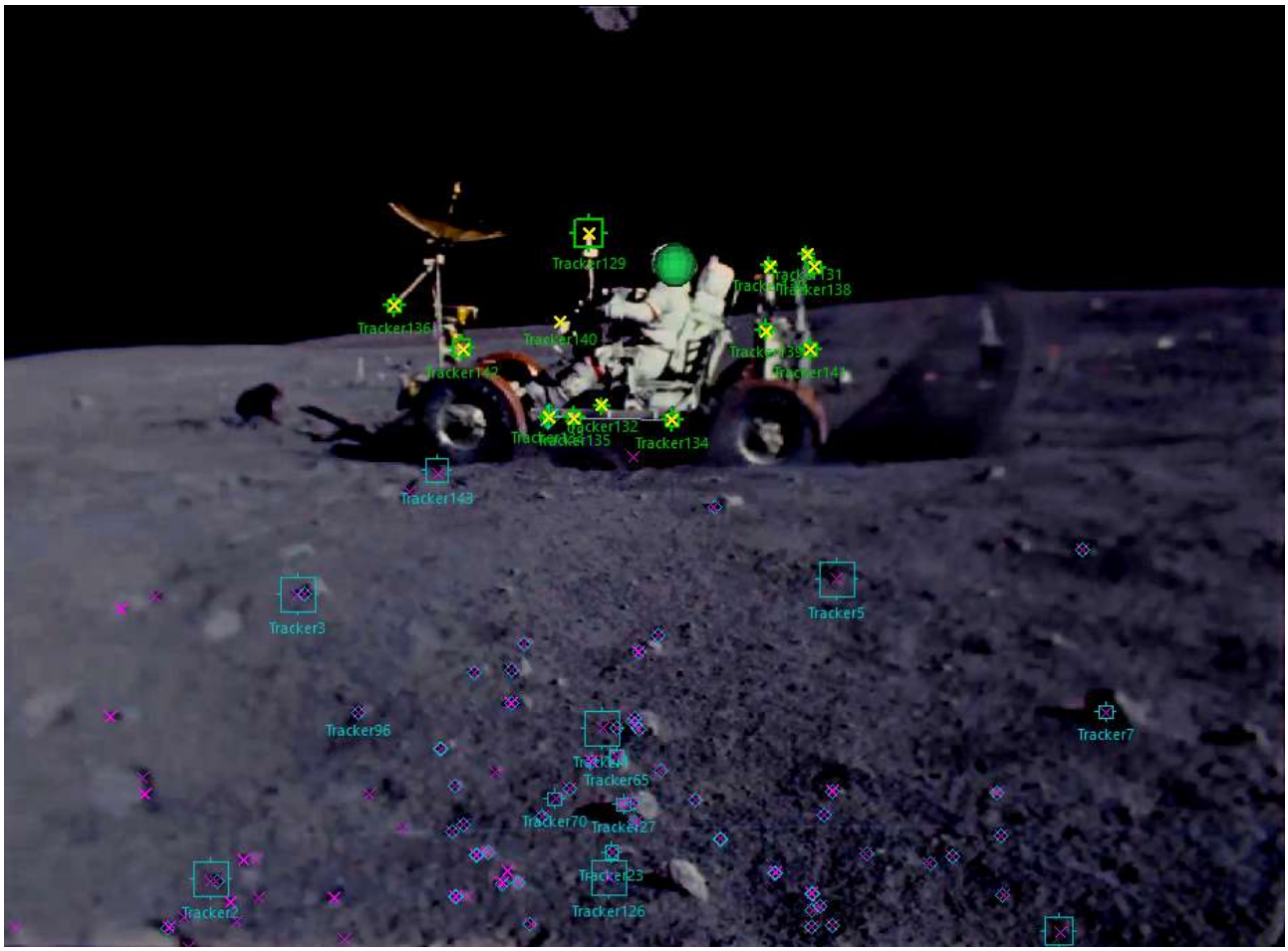

Figure 7 – 3D Analysis, using SynthEyes, of the "Grand Prix" sequence of Apollo 16: trackers.

The graphs developed by SynthEyes starting from the Andersson preset analysis (figures 8, 10, 11) represent the movement of the Rover and the DAC Camera in the 3 dimensions describing the relative motions of the system within the sequence which contains, at frames 21-57, the images studied by Horanyi and Hsu.

[7] *https://www.ssontech.com/content/apollo.html Apollo Rover Practice Shot © 2003–2019 Andersson Technologies LLC, Last Updated 30 May 2019* [*Ann. 9* - *Ann. 10*]

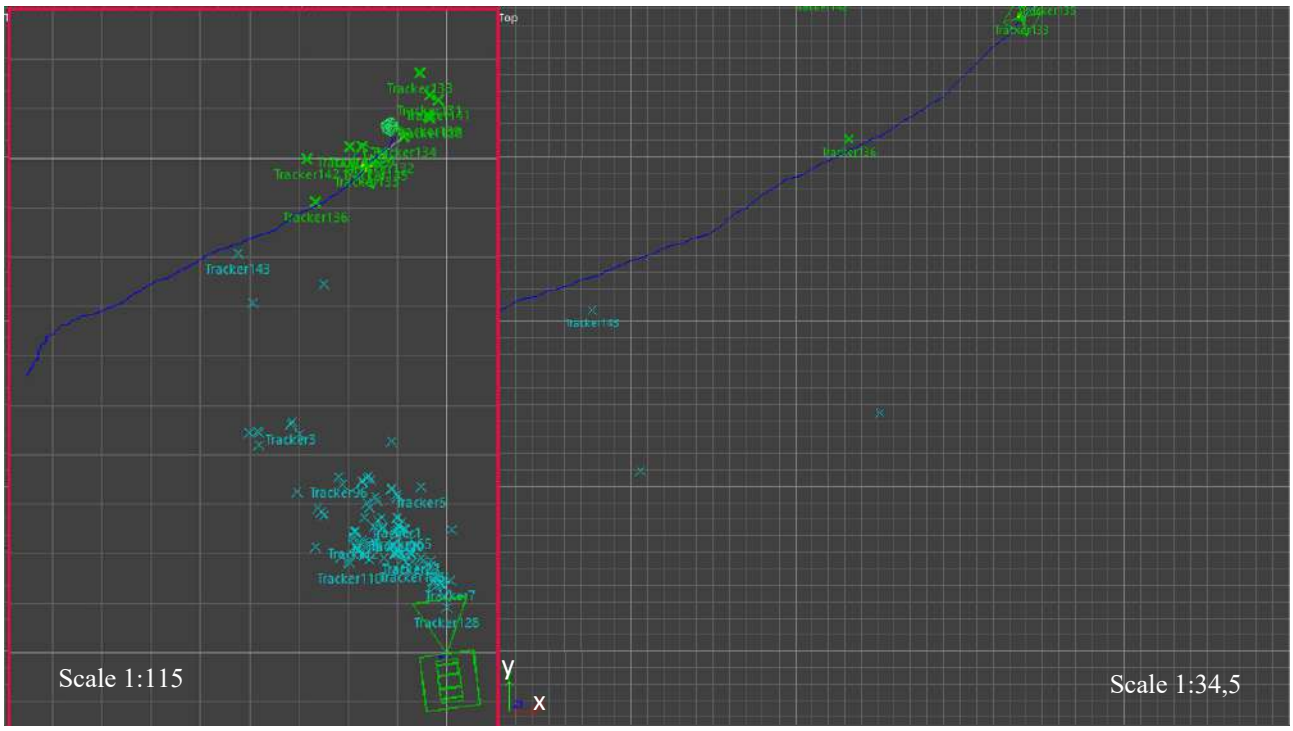

Figure 8 – 3D Analysis, using SynthEyes, of the "Grand Prix" sequence of Apollo 16: view of LRV motion from the top

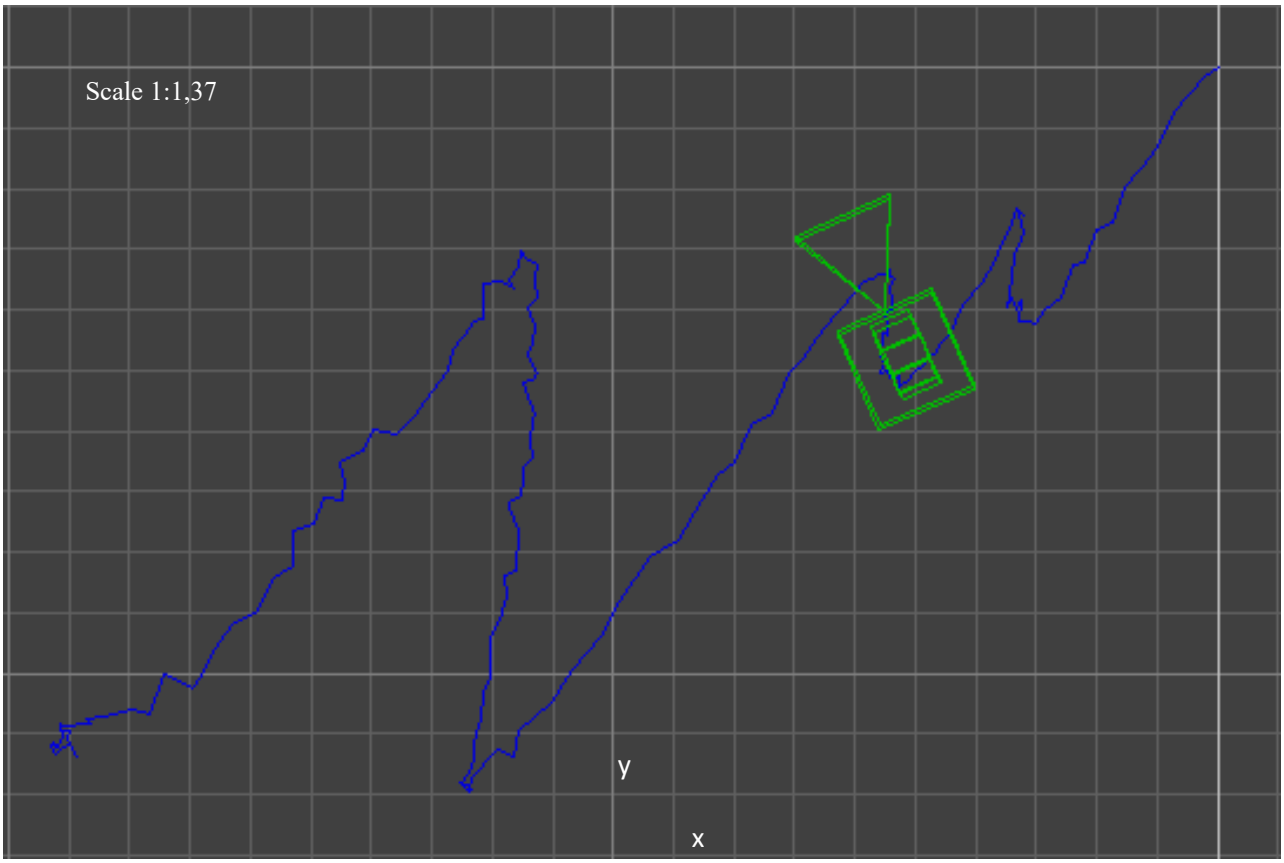

Figure 9 – 3D Analysis, using SynthEyes, of the "Grand Prix" sequence of Apollo 16: view of DAC motion from top

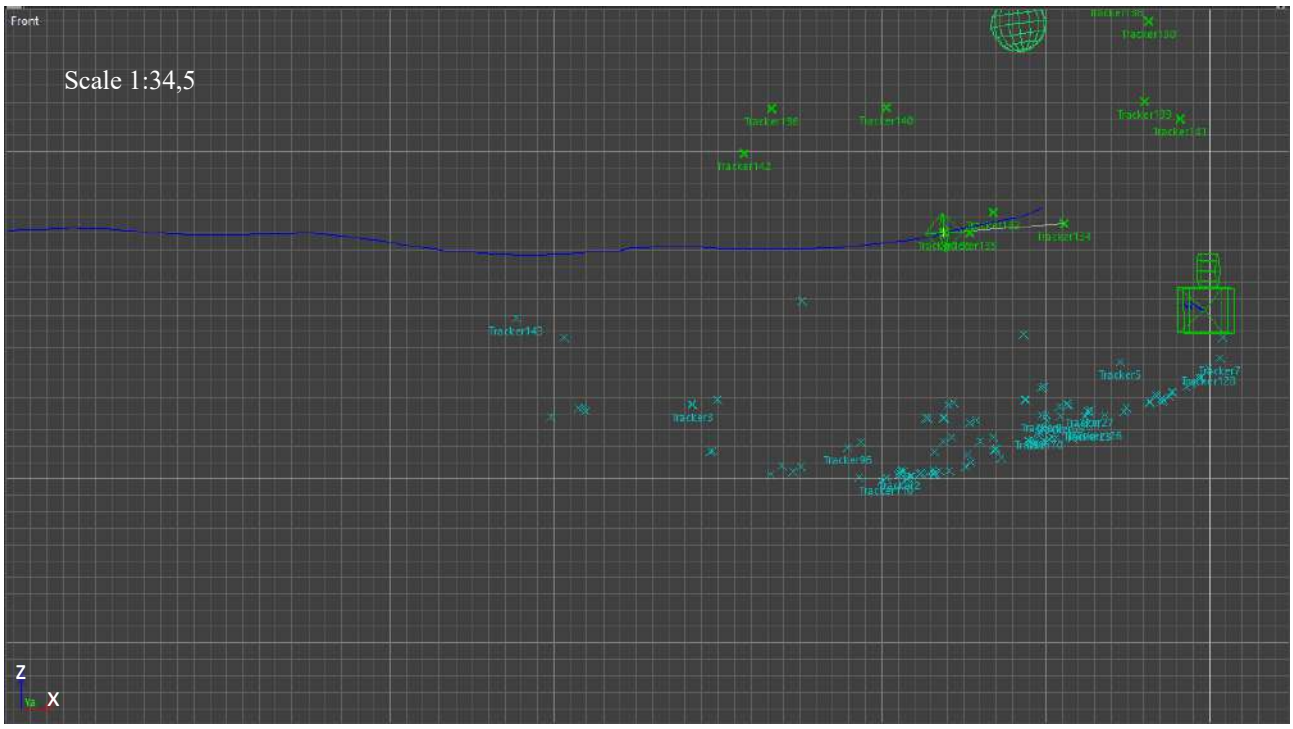

Figure 10 – 3D Analysis, using SynthEyes, of the "Grand Prix" sequence of Apollo 16: front view of LRV motion

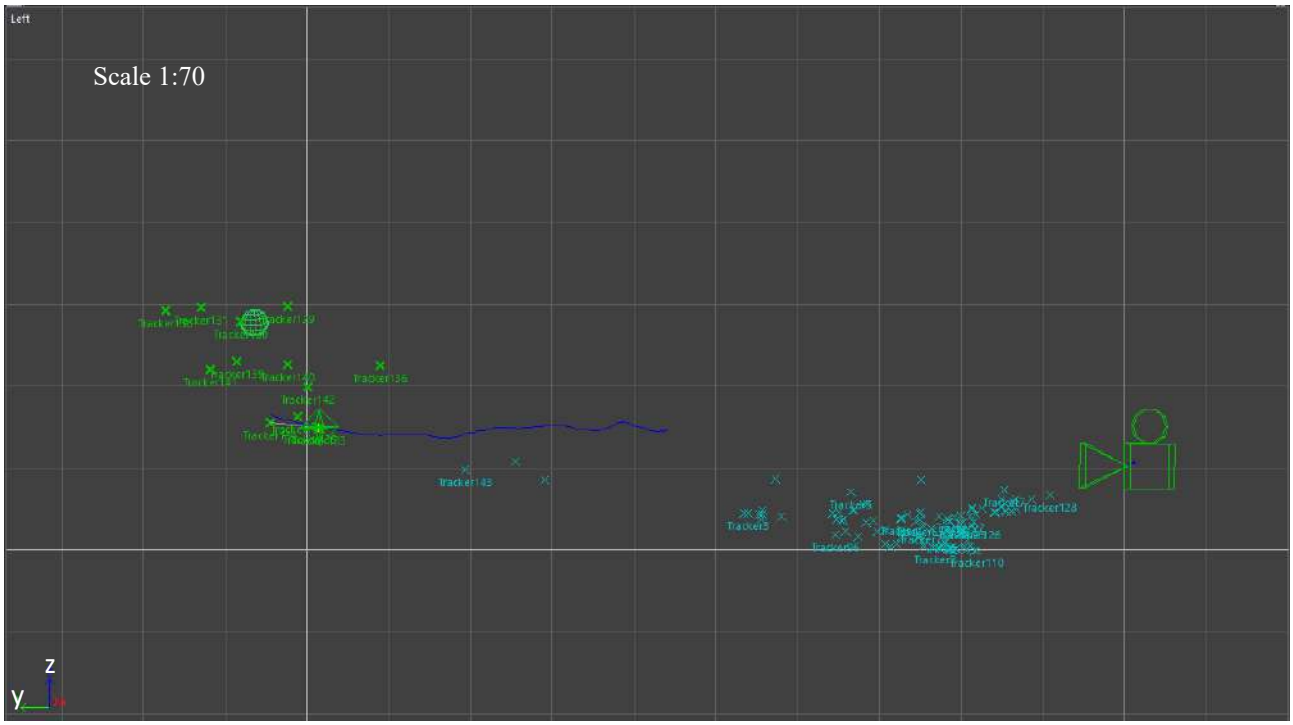

Figure 11 – 3D Analysis, using SynthEyes, of the "Grand Prix" sequence of Apollo 16: side view of LRV motion

As a first element of analysis, it is necessary to underline the motion of the camera, clearly visible in detail from the top view (figure 9), although the overall path it has made does not exceed 30 cm. The motion of the Maurer DAC, in addition to drawing a zigzag on the XY plane, consists of a rotation in the same direction as the motion of the Rover, a circumstance justified by the understandable need of the astronaut Charles Duke, who handled it, to follow the subject of filming.

The second element of the system that can be deduced from the SynthEyes graphs, in this case macroscopic, is the approach of the Rover to the camera on the Y axis during the examined sequence (figure 11).

As will be understood, both elements contribute to weakening the model proposed by the Colorado University team. This model evidently does not take into account the motion of the observer, nor does it identify the correct direction of motion of the LRV in space, simply assuming as an initial hypothesis that the vehicle speed vector is orthogonal to the plane of view. In conclusion, given the observations made so far, we can affirm that a two-dimensional model is not able to correctly represent the relative motions of the bodies within the system.

Finally, it's worth formulating two other important questions regarding the proposed results to which the cited paper does not seem to give sufficient answers.

The first on **measurement accuracy:** is the propagation of the error proposed by Horányi and Hsu correct? How the errors of X_0 and $Z_{0,}$ as well as V_{X0} and $V_{Z0,}$ are calculated?

The second question that still remains open regards the consistency of results. At the end of the paper, we read: "*The fact that our measurements show no deceleration in the X-direction (see the right panel of figures 3 and 4) confirms that the footage was recorded in an airless environment".*

But what and how much data confirm the conservation of speed? Are those collected sufficient? The lack of tracking for the descending trajectory of the dust does not allow us to verify alternative hypotheses. Beyond the presentation of the graphs, no statistical evidence is cited to support this statement.

SECTION A
Big Navy Salute

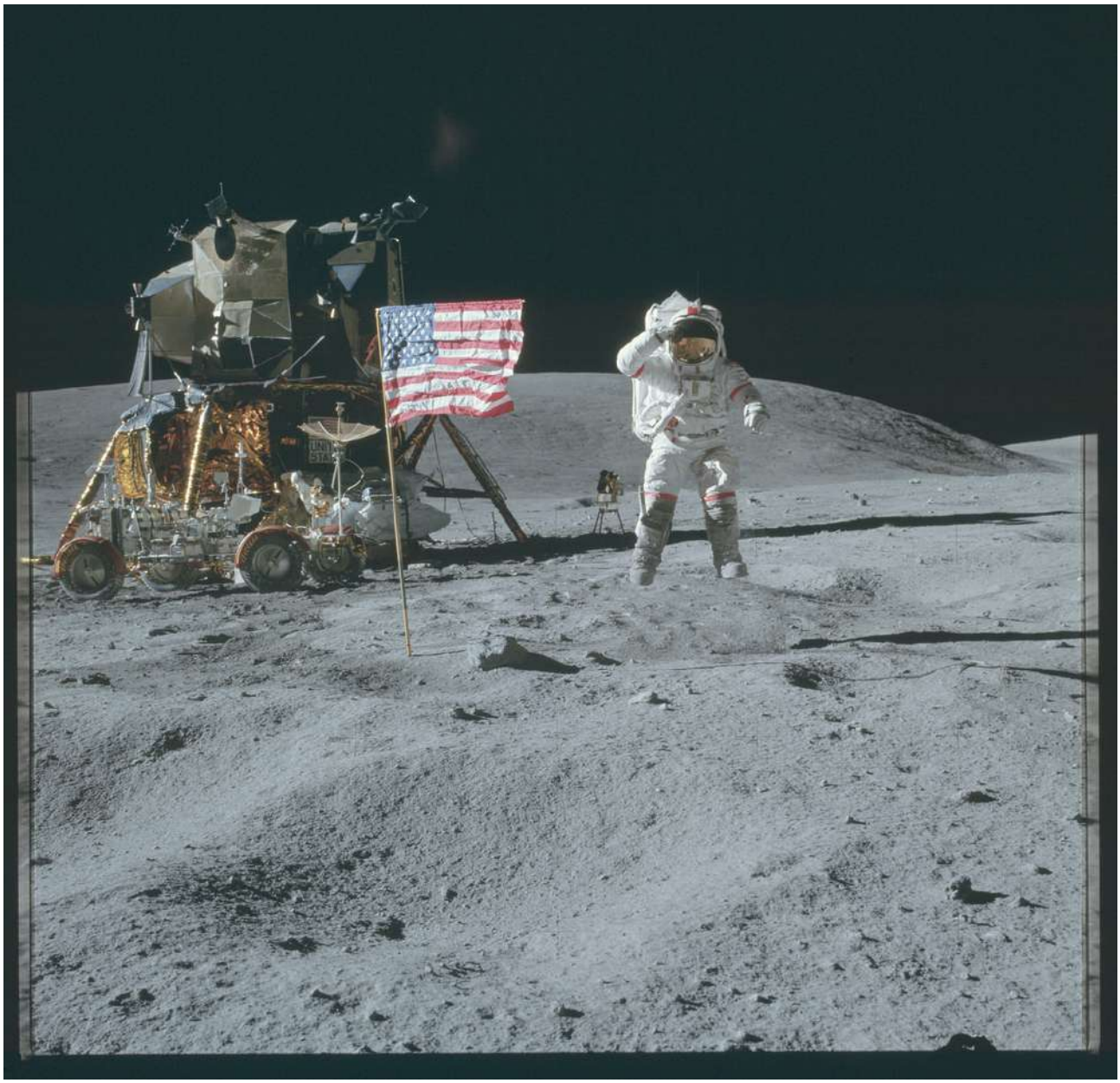

Figure A1 – J.W. Young salutes the flag, AS16-113-18339 [8]

A.1. APOLLO 16 [9]

Apollo 16 was the tenth manned mission of NASA's Apollo program, the fifth and at the same time the penultimate mission to bring humans to the moon. It was successfully concluded by reaching the main goal of the mission which, in fact, was the fifth moon landing.

The crew consisted of Commander John W. Young, the lunar module pilot Charles M. Duke, and the command module pilot Thomas K. Mattingly (the only one not to descend on lunar soil). The

[8] *https://www.hq.nasa.gov/alsj/a16/images16.html Apollo Image Library, Apollo 16 Figure Captions Copyright © 1996-2017 by Eric M. Jones, last revised 16 March 2019.*

[9] *https://www.nasa.gov/missions/apollo/apollo-16-mission-details/ National Aeronautics and Space Administration. Last Updated Sep 29, 2023*

mission began with the launch of the two Apollo 16 modules via the Saturn V rocket from the John F. Kennedy Space Center on 16th April 1972. The moon module landed on 21st April 1972 at 02:23:35 UTC on the Descartes Highlands. The astronauts spent 71 hours, 2 minutes, and 13 seconds on the surface of the Moon, of which 20 hours 14 minutes, and 14 seconds were engaged in Extra Vehicular Activities. During these activities, a total of 95,8 kg of moon rocks were collected. On 27th April 1972, at 19:45:05 UTC, Apollo 16 dived into the Pacific Ocean.

A.1.1 ALSEP Off-Load

21st April 1972 is the day after man's 5th moon landing. Astronauts wake up on the Orion lunar module and are preparing to fit out the EVA 1. They will be engaged in some activities before leaving to explore the Descartes Highlands. Among these, is the activation of the Lunar Rover and the ALSEP scientific unit.

The Apollo Lunar Surface Experiments Package (ALSEP) comprised a set of scientific instruments placed by the astronauts at the landing site of each of the five Apollo missions from 12 to 17. After successfully deploying one of the probes, Commander John Young inadvertently caught his foot on the cable to the experiment from the Central Station. The cable was pulled out of its connector on the Central Station. Although some technicians and astronauts on Earth believed that a repair was feasible, mission control ultimately decided that the time necessary for a repair could be put to better use on other work, and so the experiment was terminated. [10]

Before leaving the moon landing site for EVA 1, John Young and Charlie Duke also planted the U.S. flag in the lunar soil.

A.1.2 DESCRIPTION OF THE SEQUENCE [11]:

Astronaut John W. Young, commander of the Apollo 16 lunar landing mission, leaps from the lunar surface as he salutes the United States flag at the Descartes landing site during the first Apollo 16 extravehicular activity (EVA). Astronaut Charles M. Duke Jr., lunar module pilot, took two pictures for two different jumps. The Lunar Module (LM) "Orion" is on the left. The Lunar Roving Vehicle (LRV) is parked beside the LM. The object behind Young (in the shade of the LM) is the Far Ultraviolet Camera/Spectrograph (FUC/S).

A.1.2.1 Sources: The images used for this study come from Apollo 16 Journey to Descartes, complete TV and onboard film © 2005 Spacecraft Film (courtesy NASA). The sequence "Salute to the Flag" is published at this link: https://youtu.be/sBta1iBE2NU [*Ann. A1*]

A.1.2.2 Other official sources containing the same sequence:

- Apollo 16 Lunar Surface Journal Corrected Transcript and Commentary by Eric M. Jones 1996, *Revised 24th April 2017.* https://www.hq.nasa.gov/alsj/a16/a16salute.mpg [*Ann. A2*]
- "Nothing so Hidden" Published by NASA on 12th July 2018 https://plus.nasa.gov/video/apollo-16-nothing-so-hidden-2/

A.1.2.3 Chronology and dynamics of motion [12]

120:25:42 *Duke: "Come on; a little bit closer. Okay, here we go. A big one".*

---

[10] *http://www.lpi.usra.edu/lunar/missions/apollo/apollo_16/experiments/as/ Apollo 16 Mission Science Experiments - Active Seismic, Lunar and Planetary Institute*

[11] *https://www.nasa.gov/image-article/john-w-youngs-lunar-salute/ NASA, John W. Young's Lunar Salute, Last Updated: Sep 23, 2022, Responsible NASA Official: Abigail Bowman*

[12] *https://www.hq.nasa.gov/alsj/a16/a16.alsepoff.html Apollo 16 Lunar Surface Journal Corrected Transcript and Commentary by Eric M. Jones. Revised 24th April 2017.*

John bends his knees slightly, springs about a half meter off the ground, and salutes. He is off the ground about 1.45 seconds which, in the lunar gravity field, means that he launched himself at a velocity of about 1.17 m/s and reached a maximum height of 0.42 m. This superb picture is AS16-113- 18339. Note that John's total weight - body, suit, and backpack, is about 30 kilograms or 65 pounds. In Houston, Tony chuckles with delight.
Ken Glover writes: "For students interested in analyzing John's 'Big Navy Salute', I have made a short, 2.7 Mb MPEG-1 clip of better resolution and at 29.97 fps, showing only the two jumps".
Jones: "John's jumps says to me he's got a great deal of confidence this early".
Duke: "His balance was really extraordinary".

120:25:49 *Duke: Off the ground. Once more. (Pause) There we go.*
John's second jump lasts about 1.30 seconds and, consequently, his launch velocity is about 1.05 m/s and his maximum height is 0.34 m. This picture is AS16-113- 18340.
Journal Contributor Joe Cannaday notes that the peak of John's first jump was at about 120:25:49 and the peak of the second was three seconds later at 120:25:52.

Figure A2 – Second jump by J.W. Young during the salute to the flag, AS16-113-18340 [5]

A.2. IMAGE PRODUCTION TECHNOLOGY.

The images of this sequence were filmed by RCA Color TV (CTV) [13], a television camera already used in the Apollo 15 mission, and improved in its performance and functionality for Apollo 16. The camera was set up on board within the Lunar Module during the moon landing phase and then transferred to the Lunar Rover (or in some cases on a tripod) for the shooting of Extra Vehicular Activities. It integrated the Ground-Controlled Television Assembly (GCTA), which allowed the Huston Mission Control Center a remote control in real time (on, off, pan, tilt, zoom, diaphragm opening and closing f / 2.2 - f / 22, lighting control) [14]. The machine was fitted with a photomultiplier tube which contained a 16 mm sensor, equipped with a technology that RCA was developing just in that period, the Silicon Intensifier Target Tube [15], capable of a great sensibility; it was also suitable for shooting very shady areas, and it could resist to strong sun exposure without being damaged. Sensibility was electronically adjusted within the range of 1 - 1000 lux [16]. The optical group allowed a zoom range of 12,5-75 mm and the possibility to vary the angle of view from 54° to 9° [7].

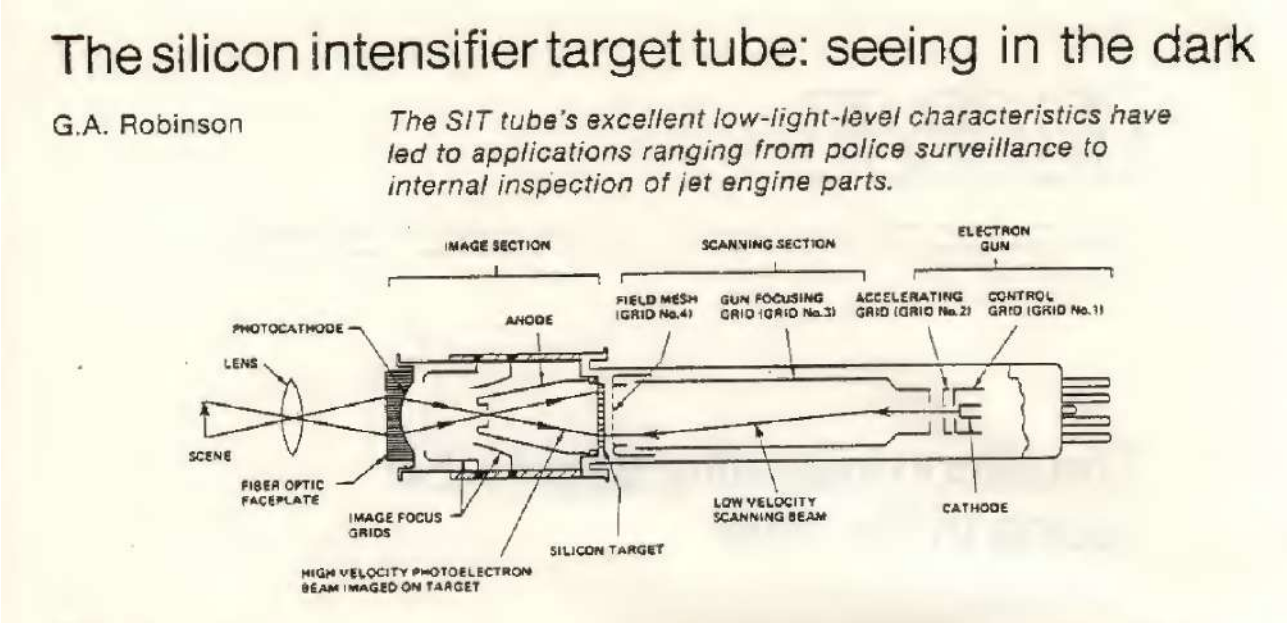

Figure A3 – Functionality scheme of SIT Camera Tube RCA

The mechanics allowed a scan rate of approximately 30 fps (exactly 29.97 fps) with 525 scan lines per frame, in line with the standard NTSC of American commercial television. More exactly, 60 interlaced fields (semi-frames) were produced sequentially every second with a resolution of 200 TV lines per image and with an image proportion of 4:3.

The machine was able to produce colour images thanks to a simple additional device developed by CBS from the '40s (Col-R-Tel), consisting of a rotating disc with red, green, and blue filters, placed

---

[13] https://tothemoon.ser.asu.edu/files/apollo/apollo_16_lunar_photography.pdf *Apollo 16 Lunar Photography, NASA – National Space Science Data Center, Greenbelt MD 1973* [Ann. 3]

[14] https://www.nasa.gov/wp-content/uploads/static/history/alsj/GCTA-Manual.pdf *RCA Government and Commercial Systems, Astro-Electronics Division, Princeton NJ 08540; Issued 24 May 1971, Revised January 1972* [Ann. A3]

[15] *RCA-Norbain Electro - Optics Ltd. Seminar Electro - Optics/Laser Intern. Brighton 23-25 March 1982* [Ann. A4]

[16] https://www.nasa.gov/wp-content/uploads/static/history/alsj/Shooting-Moonwalks.pdf *"Shooting the Apollo Moonwalks" By Sam Russell RCA project engineer of GCTA color television camera, Apollo missions 15 -17* [Ann. A5]

in front of the tube sensor. The disk made a turn in exactly one-third of the scanning frequency, thus producing 3 half-frames of different colours every twentieth of a second.

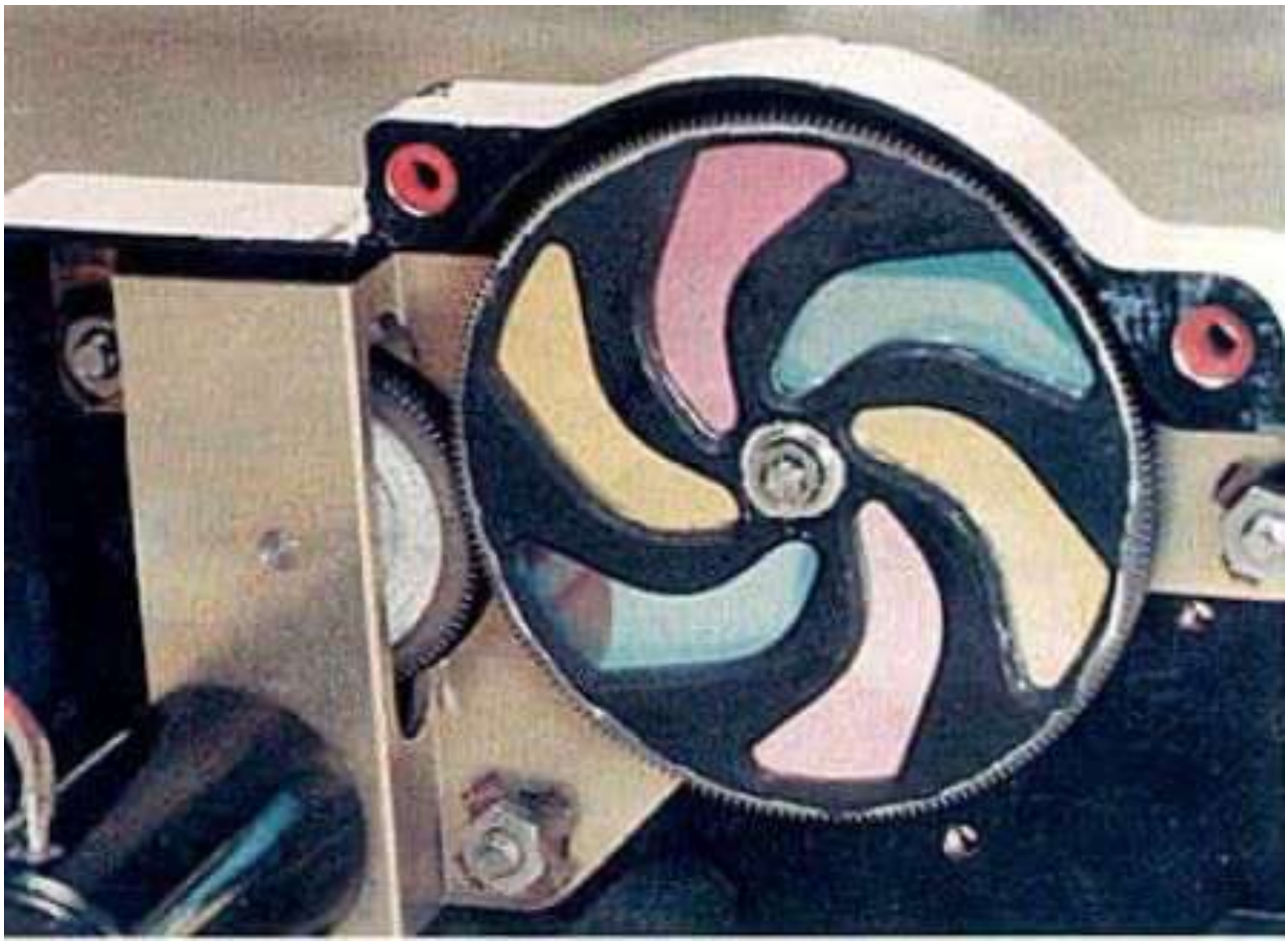

Figure A4 – The Field Sequential Colour Wheel (Col-R-Tel) conceived by CBS (Lebar, 1997, p. 52.)

When the CTV was installed on the Rover, the images were sent via radio through the Lunar Communications Relay Unit (also developed by RCA), which allowed the direct connection between the Rover and the receiving stations on Earth. The Rover was therefore equipped as a completely independent mobile unit, capable of transmitting directly to the ground even when it was parked miles away from the lunar module. However, this required operations of new antenna pointing every time the vehicle was parked.

A.2.1 Estimate of the geometric aberration of the images

The electronic photomultiplier of the camera (RCA Vidicon SIT Tube) required a spherical photocathode surface and, following the transition from a flat image to a curved surface, the geometric distortion increased by a typical value of 2% compared to traditional optical groups, with a pincushion effect [8]. The use of long focal lengths (which produced narrow field angles) would certainly have increased this limit of linearity characteristic of the camera, again in the sense of the pincushion, while at short focal lengths (wide angle) there could have been a recovery, or more likely a mix between the pincushion and the so-called barrel distortion.

The spatial measurements of the sequence in question were carried out in the central area of the images, where the two types of distortion are in any case almost irrelevant. However, for greater

accuracy of the measurement system, it was considered appropriate to calculate the geometric distortion anyway.

A.2.1.1 Calculation of the focal length used for shooting.

From the high-resolution images AS16-113-18339 and AS16-113-18340 (figures A1 and A2) we can draw fundamental information on the "set" in which the sequence was shot. The image *AS16-113-18340*, taken with a 60 mm lens [6] (for this reason not subject to appreciable geometric aberrations), shows on the back the LR with the CTV in activity. All we need to do is identify the distance between the lens and the subject in order to determine the focal length using the conventional formulas of photographic optics.

Through a perspective analysis made with the Adobe Photoshop CS6 Vanishing Point Filter [17], determining the distance between the target and the astronaut John Young is quite simple. By identifying the vanishing points, this filter enables the construction of reference planes that characterize the perspective development of the image, thereby allowing for accurate measurements of the three-dimensional space.

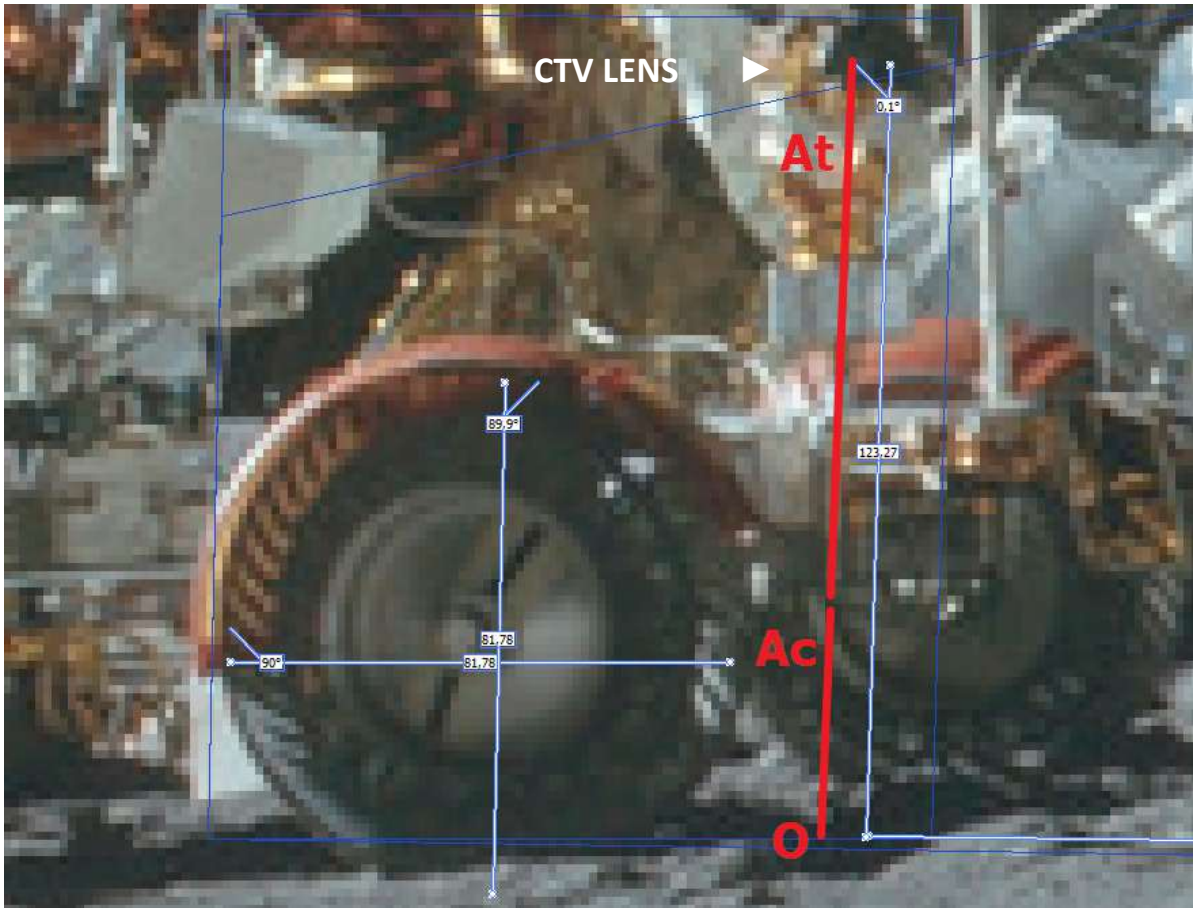

Figure A5 – AS16-113-18340, measurement system calibration with Adobe Photoshop CS6 Vanishing Point Filter

[17] https://helpx.adobe.com/uk/photoshop/using/vanishing-point.html *Adobe Photoshop User Guide, Image transformations, Vanishing Point Copyright © 2019 Adobe 345 Park Avenue San Jose, CA 95110-2704*

A.2.1.1.1 Relevant known dimensions.

The known dimensions through which it is possible to set up a measuring system can be obtained from the diameter of the wheel of the LR [18] (cm 81,8). The wheel allows to have a reference measurement both in height and in width. Some dimensions of objects in the foreground are known (PLSS Unity and OPS Module): a perspective analysis of the space represented by the photo is therefore possible.

Let's set as the origin of our system O the projection of the CTV Camera lens to the ground. We indicate with At and Ac respectively the height of the CTV on the chassis and the height of the chassis from the ground in the absence of load [11] (the thickness of the chassis is also considered); finally, Y indicates the position on the ground of John Young.

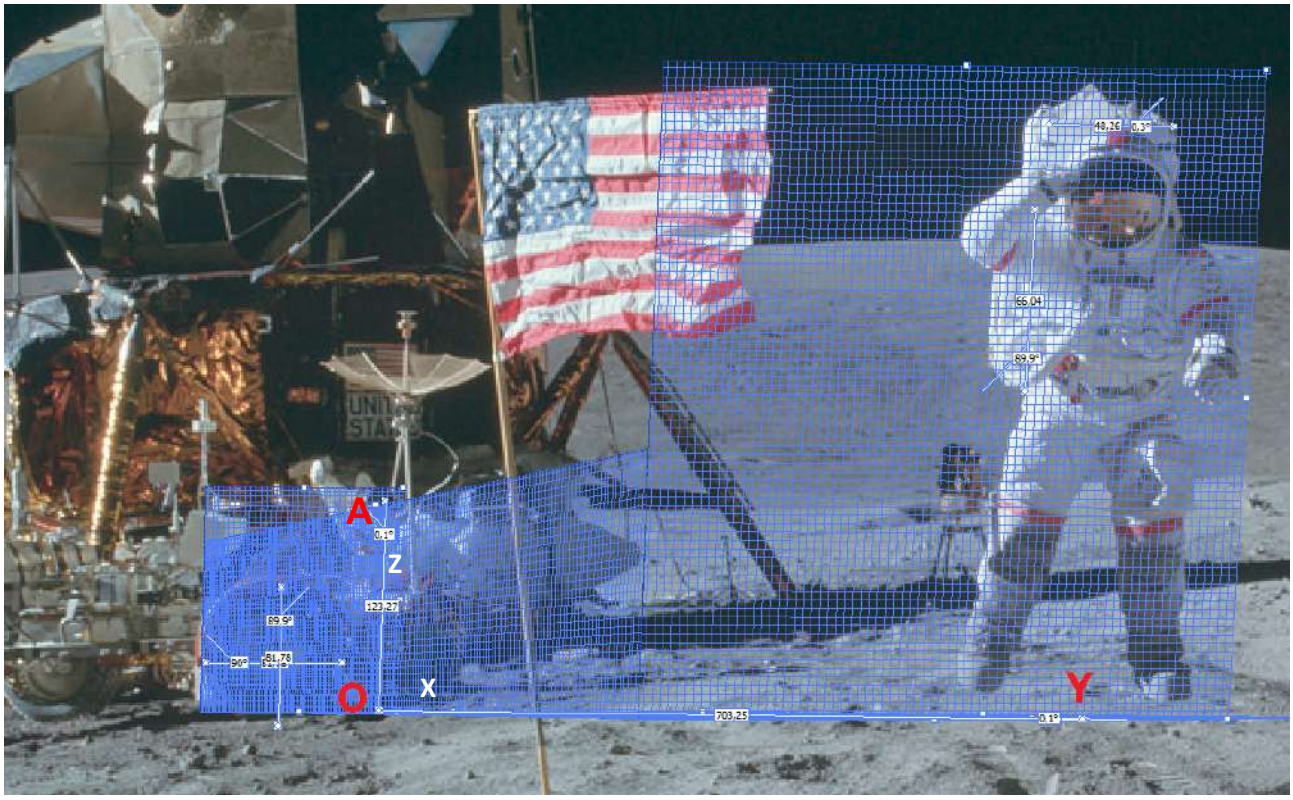

Figure A6 – AS16-113-18340, Distance of John Young from the lens

The following measures are known:

- The diameter of the Rover wheel is 81,8 cm (32,2 in.) [15]
- The height of the camera from the ground A can be derived as: $A = A_t + A_c$ = 123 cm (48,41 in.) [15]
- The height of the Training PLSS Unity (Portable Life Support System) worn by John Young is 26 inches, thus 66,04 cm (module OPS not included) [19]
- The width of module OPS (Oxygen Purge System) of John Young is 19 inches, thus 48,26 cm [12]

The line of contact of the wheel of the LR with the lunar ground traces the base of the main plane for the height of which we will rely on similar points having the same quotes on the circumference

---

[18] https://www.nasa.gov/wp-content/uploads/static/history/alsj/LRV_OpsNAS8-25145.pdf *Lunar Roving Vehicle Operation Handbook, The Boeing Company, Huntsville (Alabama, USA) April 19, 1971* [Ann. A6]

[19] *Measurements of Apollo 16 Training Unit, Courtesy Dean Eppler, NASA, Lyndon B. Johnson Space Center, Houston Texas, USA. PLSS Unity measurements do not include the OPS module positioned above.*

of the wheel itself. There is only one vertical plane that allows us to make the measurements of the wheel diameter in width and height concordant: once identified, this will allow us to correctly express the perspective. Once the main (vertical) plane has been identified, the Photoshop CS6 Vanishing Point tool allows us to derive planes that are orthogonal to each other. We can therefore proceed to derive the plans allowing us to connect the shape of the astronaut in the foreground with the objects whose measurements have been calibrated in the background: the measurements of the PLSS Unity and the OPS Module that we can check on the new frontal plane built, exactly match those known. At this point, we can derive the horizontal (or ground) plane on which we detect the sought distance.

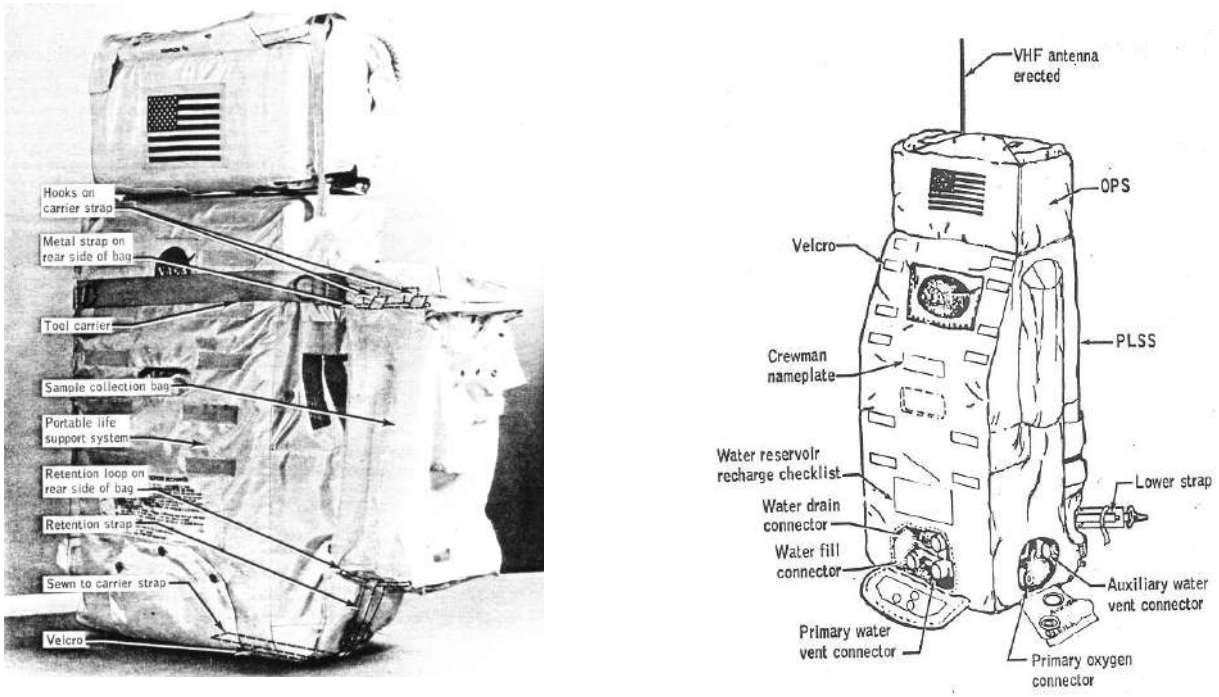

Figure A7 – Apollo 16 Training PLSS Unity and OPS Module

A.2.1.1.2 Measurement result

Using the metric system just defined, the distance OY results to be: 703,25 cm. The instrumental error relating to the Prospective Filter of Adobe PS CS6 is +/- 1.5 pixels, as we will demonstrate in C.3.7. On the just measured distance, this error is 4,33 cm X 1,5 = 6,49 cm. Definitely, the result of the measurement is:

OY = 703 cm +/- 6,5 cm

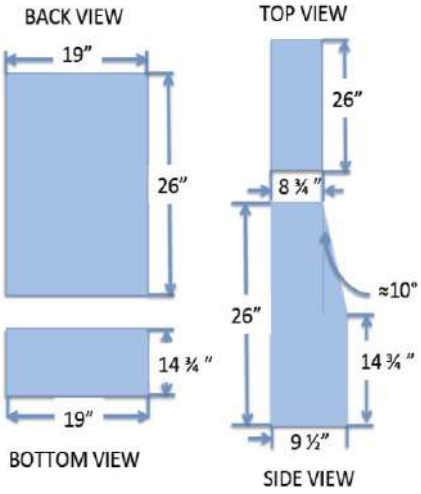

Figure A8 – Apollo 16 Training PLSS dimensions

A confirmation of the correctness of the investigation carried out comes from the planimetric map developed by Brian McInall and published by NASA at the following address:
https://www.nasa.gov/wp-content/uploads/static/history/alsj/a16/A16ALSEP-DeploymentPlanimetricMapLROC-M175179080LR_Jan2017.jpg [20]

[20] https://www.hq.nasa.gov/alsj/a16/a16.alsepoff.html *Apollo 16 Lunar Surface Journal Corrected Transcript and Commentary by Eric M. Jones. Revised 24 April 2017*

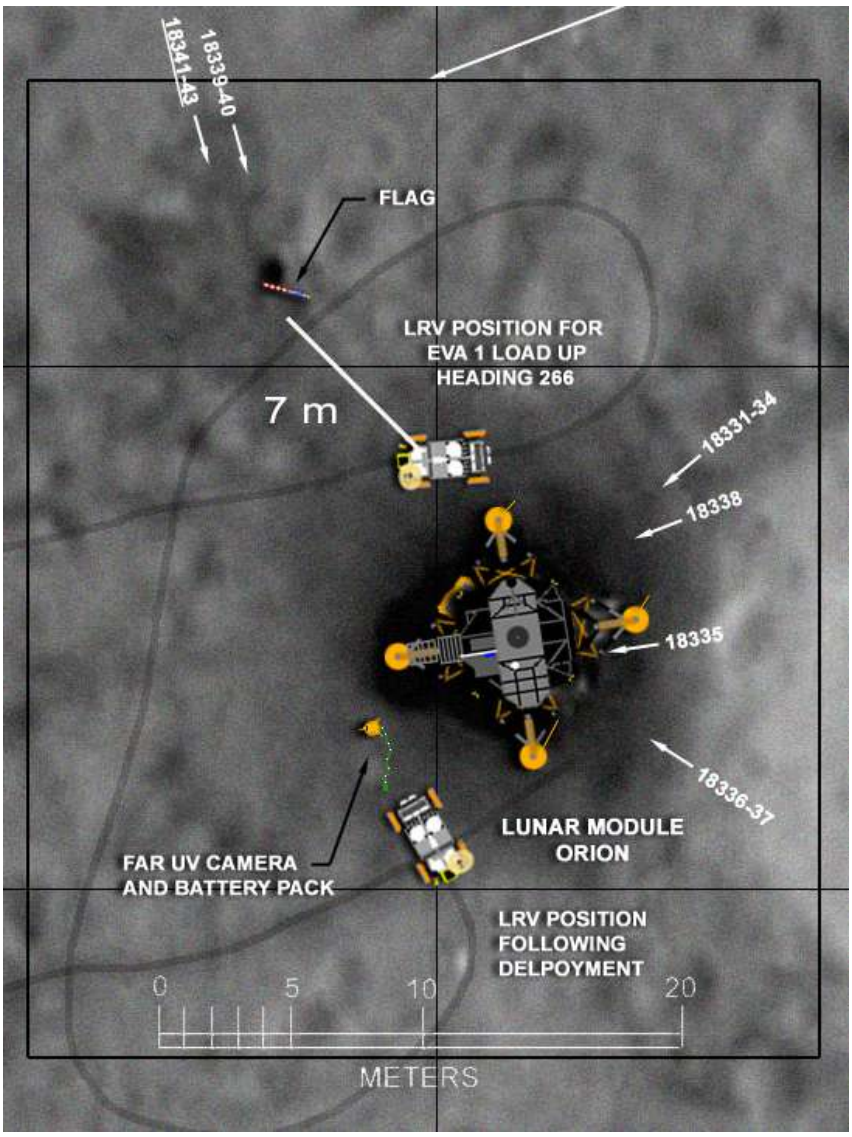

Figure A9 – Extract of the planimetric map of the ALSEP area of Apollo 16, produced by Brian McInall

Given the metric scale of the map with a simple measurement (always carried out with Adobe PS CS6) it is possible to confirm the experimental data just obtained starting from high-resolution photography AS16-113-18340.

A.2.1.2 Conclusions on the calculation of the focal length used for the recovery

By indicating PLSSctv as the height of the PLSS Unity on the CTV sensor and PLSSr as its real value, the focal F used is given by the relation F = OY x $PLSS_{ctv}$ / $PLSS_{r.}$ In fact, even if the optical group of the camera was more complex, we can simplify it according to the classic scheme:

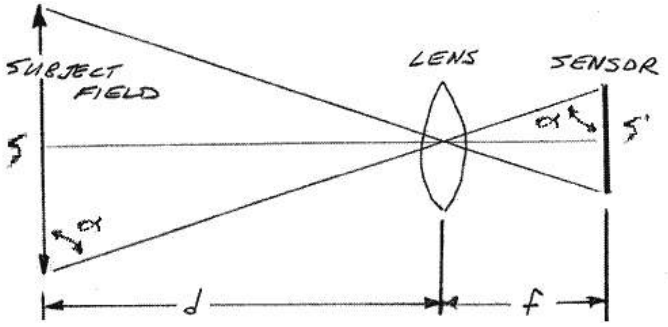

$$d = \frac{1}{2} S * \tan(\alpha)$$

$$f = \frac{1}{2} S' * \tan(\alpha)$$

then

$$f = d * \frac{S'}{S}$$

Figure A10 – Relationship between focal length and object size on the sensor

By opening one of the images in the study sequence with Adobe Photoshop and setting the sensor dimensions [6] (12,8 x 9,6 mm) as reference dimensions we can detect $PLSS_{ctv}$ = 2 mm with an instrumental error of 1 pixel equivalent to +/- 0,05 mm

Consequently, we obtain: F = 7030 x 2 / 660 = 21,30 mm (+/- 0,73 mm)

To evaluate the percentage of distortion to be applied based on the focal length used, it is necessary to express the latter in terms of "equivalent focal length" F_e, comparing it to a standard sensor (36mm X 24mm full-frame, known as 35mm) instead of the sensor of 16 mm with which the scene was filmed. If D is the diagonal of the 16 mm sensor and D_s is the diagonal of the standard format (43.3 mm), then:

$F_e = F \times D_s / D = 21,30 \times 43,3 / 16 = 58$ mm (+/- 2 mm)

A.2.2 Conclusions on the geometric aberration of the images

The equivalent focal length identified is between 56 and 60 mm and therefore does not involve further geometric distortion: the correction to be made to the images will only consider the typical distortion of the CTV, estimated at + 2% (pincushion) due to the spherical photocathode.

A.3. IMAGE PROCESSING ON EARTH

The real-time processing sequence for the videos arriving from the lunar surface, for Apollo 16 and 17 was the following [21]:

1. Signal reception at one of the Apollo MSFN ground stations. Filtering of video data, compensation of the Doppler effect, and its transmission to the Houston Mission Control Center.

2. Signal conversion with sequential colour fields into NTSC simultaneous colour fields by means of the RCA Scan Converter installed in Houston. Transfer of the converted NTSC signal to the Image Transform company, North Hollywood - California.

3. Reduction of video noise and image improvement through filters. Transfer of the cleaned video to Houston via microwave, for recording and immediate release to the media.

4. Recording of the film on 16 mm film by means of a colour Kinescope [22] at 29,97 fps

---

[21] https://www.hq.nasa.gov/wp-content/uploads/static/history/alsj/ApolloTV-Acrobat5.pdf *"Apollo Television" Copyright 2005 By Bill Wood, former Apollo MSFN station engineer* [Ann. A7]

[22] https://tothemoon.ser.asu.edu/files/apollo/apollo_16_lunar_photography.pdf *Apollo 16 Lunar Photografy, NASA – National Space Science Data Center, Greenbelt MD 1973* [Ann. 3]

A.3.1 Signal management at MSFN stations.

The three main earth stations of the MSFN Manned Space Flight Network, Honeysuckle Creek and Parkes in Australia, Goldstone in California, and Madrid in Spain, managed the sequential colour signal without converting it, then sent it to Houston via satellite and microwave connections. The stations that gave more coverage were the Australian one and Goldstone, California. In these stations, the frequencies 1.024 MHz (vocal subcarriers) and 1.25 MHz (subcarrier for biomedical telemetry) were removed from the FM S-band. The resulting video was then sent to the Mission Control Center in Houston. The sequence of the "Big Navy Salute" was received from the Madrid station, which represented the best tracking at that moment, in 1,284 seconds. From there it reached Houston in 0.074 seconds. [23]

John Saxon, who was Operations Manager at the Honeysuckle Creek Tracking Station during Apollo 16, writes "Honeysuckle usually communicated via microwave to a mid NSW ground station at Ceduna (South Australia), then via a pacific (geostationary) satellite to the San Francisco area, then various microwaves to/from Houston - via Goddard switching centre in Maryland. But occasionally we would use Mwave Houston to Goddard, then Atlantic satellite, then Indian Ocean satellite to Carnarvon on the (Australian) west coast to Honeysuckle. [16]

At the MSFN stations, the unconverted television transmissions from the Moon were normally recorded before the filtering operations, but later the stations themselves were asked to reuse the tapes for subsequent needs, consequently, it is not known today if such recordings still exist [17]. Before the conversion, the downlink station had the task of correcting the Doppler Shift of the lunar signal caused by the relative motion of the Earth-Moon system. Without this correction, the television circuit would have shown deformed and inverted images. The correction process was partly mechanical and partly electronic. [15]

Figure A11 - Honeysuckle Creek Tracking Station (Canberra, Australia), photo by Bryan Sullivan

[23] https://www.hq.nasa.gov/alsj/a16/a16.alsepoff.html *Apollo 16 Lunar Surface Journal Corrected Transcript and Commentary by Eric M. Jones. Revised 24 April 2017*

A.3.2 The RCA Scan Converter [24]

The cost to pay for the production of colour images was a decrease in quality. The resulting image was dark and slightly flickering. In addition, another problem arose for the RCA technicians: normal televisions could not correctly decode and display the images of the lunar camera, since these were recorded in 60 sequential red, green, and blue half-frames per second, while for the NTSC standard of the American television circuit, 30 pairs per second of semi-squares (left and right) interlaced with simultaneous colours were required. Huston solved the problem with the use of an electromechanical conversion device manufactured by RCA itself. The conversion took 12 seconds and slightly blurred the edges of the moving objects. On the moon, the RCA camera scanned one red, green, and blue video field at a time. Furthermore, the scanning proceeded according to the usual scheme used for NTSC recordings in interlaced format, thus recording a right field (or semi-frame) with 262.5 TV lines and then alternating it with a left field consisting of the remaining 262.5 lines (a total of 525 lines).

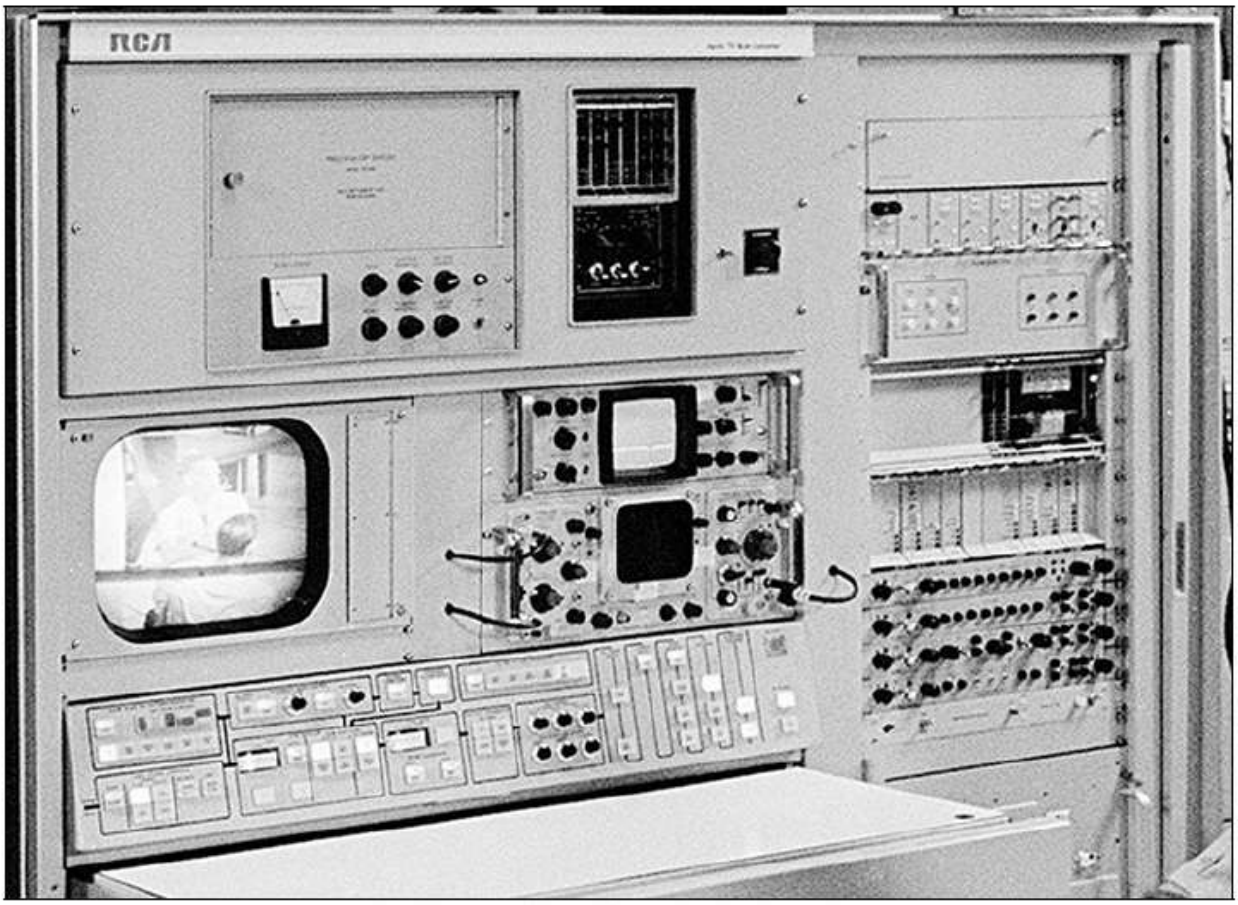

Figure 12 - Operating Console of the RCA Apollo Slow Scan Converter

The sequential production of the image fields created by the RCA "Moon Camera" can therefore be represented with the following scheme:

[24] http://www.hawestv.com/moon_cam/moonctel2.htm Copyright © 2006 by James T. Hawes

1/60 sec ↔ red field (Red) right - even (Even)
2/60 sec ↔ blue field (Blue) left - odd (Odd)
3/60 sec ↔ green field (Green) right- even (Even)
4/60 sec ↔ red field (Red) left - odd (Odd)
5/60 sec ↔ blue field (Blue) right - even (Even)
6/60 sec ↔ green field (Green) left - odd (Odd)
7/60 sec ↔ red field (Red) right - even (Even)
...

The fundamental element of the Scan Converter was the Magnetic Disc Recorder (Stock Ampex HS-100); it was an Ampex recorder used since the 60s for the slow motion of sporting events which was suitably modified to reproduce, record and delete the video fields recorded by the RCA Moon Cam on parallel tracks, in order to return as a result of 29.97 fps with 60 interlaced colour fields, through a process that was called "Moving Window".

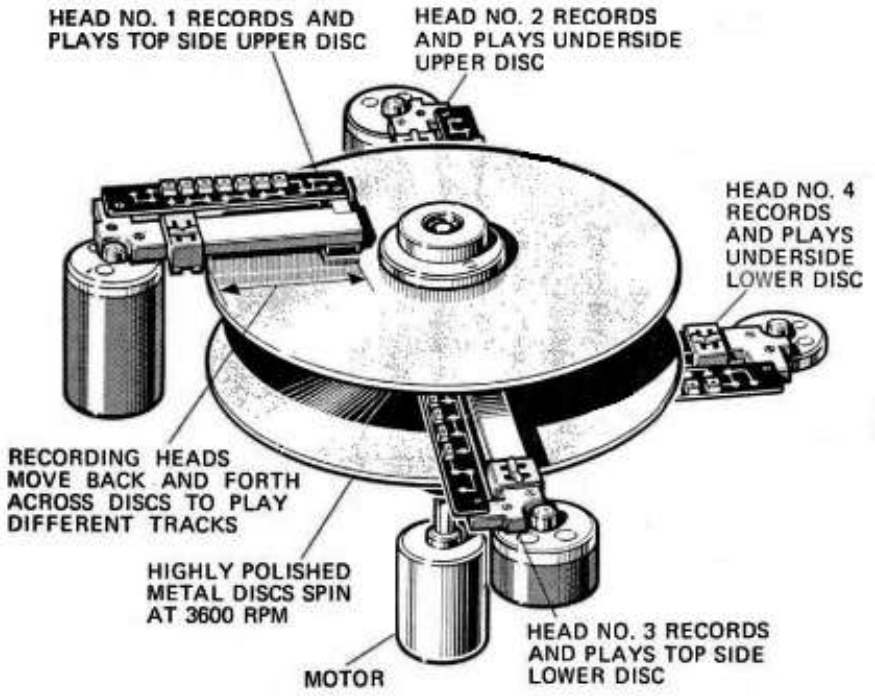

Figure A13 - Stock Ampex HS-100 disc recorder

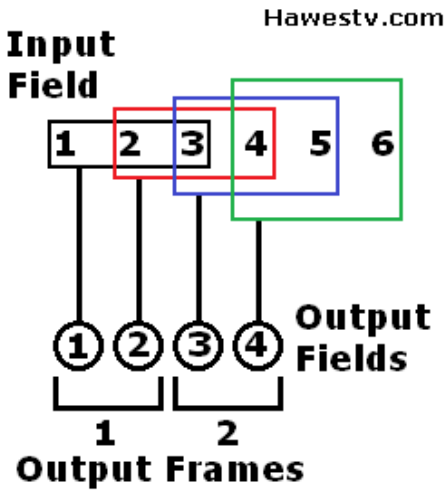

Figure A14 - The Moving Window RCA

The conversion scheme can be represented as follows:

1/30 sec ↔ 1st frame
1/60 sec ↔ $R_{even} + B_{odd \leftrightarrow even} + G_{even}$
2/60 sec ↔ $B_{odd} + G_{even \leftrightarrow odd} + R_{odd}$

2/30 sec ↔ 2nd frame
3/60 sec ↔ $G_{even} + R_{odd \leftrightarrow even} + B_{even}$
4/60 sec ↔ $R_{odd} + B_{even \leftrightarrow odd} + G_{odd}$
...
...

The conversion of the intermediate fields of each triad (from left to right and vice versa) was necessary in order to obtain perfectly interlaceable fields and it was operated through the introduction of a short delay in the recording, equivalent to the reproduction of half a TV line. From the point of view of the timeline of the events filmed in the various half-frames by the RCA CTV, each converted frame represents the superposition of 4 fields originally produced in sequence by the camera.

MOON => EARTH FRAMES **Earth Frames** **Time Keeping (s) =>**

Moon Fields	Time Keeping (s)	Colors	Interlacing	Moon Frames
-2	-2/60	Red	EVEN	
-1	-1/60	Blue	ODD	**-1**
0	0	Green	EVEN	
1	1/60	Red	ODD	**0**
2	2/60	Blue	EVEN	
3	3/60	Green	ODD	**1**
4	4/60	Red	EVEN	
5	5/60	Blue	ODD	**2**
6	6/60	Green	EVEN	
7	7/60	Red	ODD	**3**
8	8/60	Blue	EVEN	
9	9/60	Green	ODD	**4**
10	10/60	Red	EVEN	
....				....
.... **60**				.... **30**

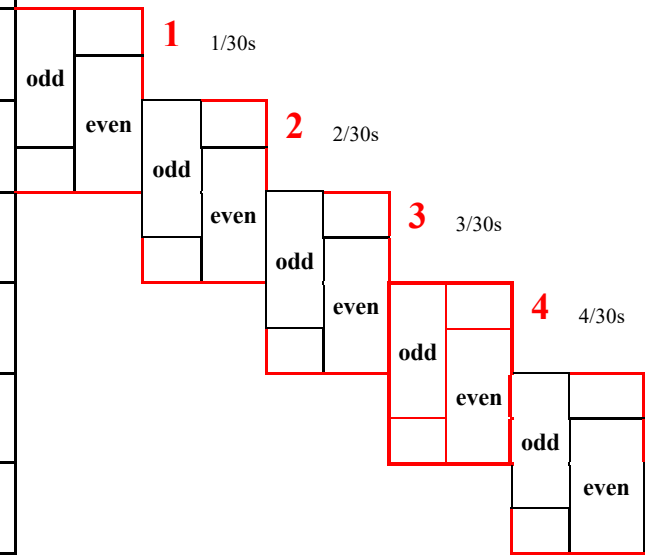

Table A1 – Comparison between the timeline of the CTV RCA and the timeline of the converted video signal

For this reason, the fast-moving objects of the sequence examined by this study in each frame present contours that highlight the colour of the last recorded field in the direction of motion. Considering the overlap of 3 fields filmed on the Moon for each half-frame of the sequence converted on Earth, the dominant colour on said contour will result in the sequence of colours
Red - Green - Blue.

Exceptions to this sequence and precession mechanisms of the dominant colours on the contours may be due to the acceleration of the moving bodies (when the speeds decrease the colours will tend to overlap), or to the different distances from the objective (the perspective analysis can explain the presence of different colours on objects closer or further away from the camera that is filming the scene).

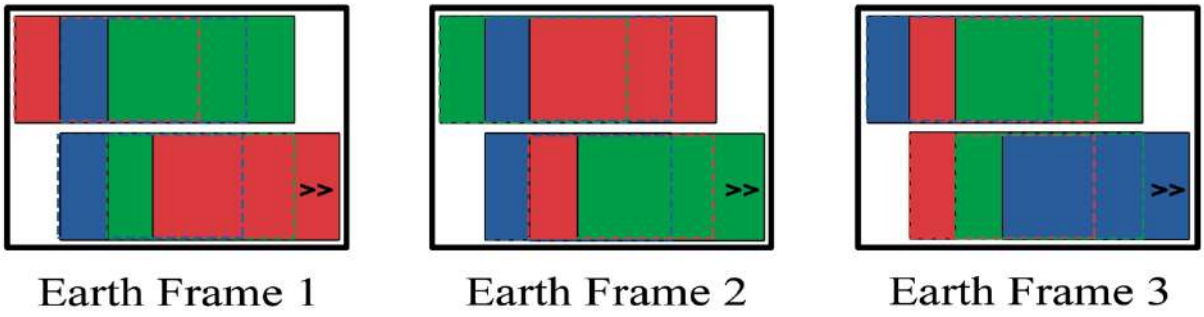

Figure A15 – Moon TV, conversion of the sequence of R-B-G-R fields taken from the CTV RCA into NTSC frames

Figure A16 – Moon TV, succession of "dominant" colours on the outlines of moving objects

Taking this frame production process into consideration is fundamental for the analysis of the sequence, and makes the exclusive analysis of the most advanced point of the body in motion reliable, since the rest of the image is nothing other than the result of 4 different events.

Once the conversion of the half-frames was completed, the video of the RCA TV camera underwent other electronic manipulation processes in Huston: luminance adjustment, chromatic carrier suppression, horizontal and vertical synchronization, chromatic signal enhancement, addition of the audio subcarrier with the mixing traces from the moon and the earth.

A.3.3 Image Transform [14]

From Huston the signal was sent to North Hollywood, California, to be processed by the Image Transform company in order to perform a "cleaning" of the images. Following the limited bandwidth availability and the various manipulations made necessary, the video presented a rather

heavy chaotic disturbance (or noise). Image Transform algorithms were able to separate motion areas from static portions of the image by comparing four frames at a time. In static image regions, noise has been reduced by a factor of four, allowing for a significant detail enhancement. The moving areas have been spatially filtered obtaining only a partial reduction of the noise. The static portions of the images and those relating to the movement have been recombined without the use of artefacts.

A.3.4 From Kinescope up to digital images

The videos that the astronauts shot on the Moon with the RCA TV Camera and that on Earth were converted to the American television standard, and were transferred onto 16 mm film for archiving, using the reference technology of the time: the Cinescope (or telerecording). With this format, they have been made publicly available, in particular for dissemination or research purposes. [15]

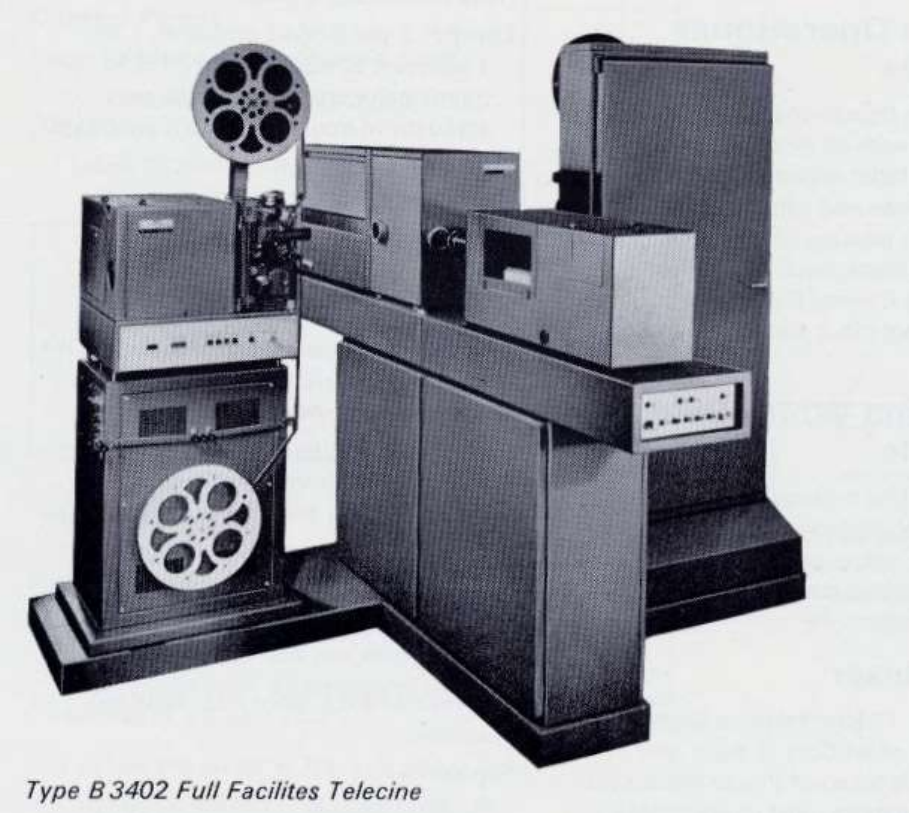

Figure A17 - Marconi B 3402 Cinescope, created in the late 60's for English TV

The Kinescope system simply consisted of the use of a precision camera aimed at the screen of a high-performance monitor: the camera, synchronized with the monitor's scanning frequency, recorded the images, and imprinted them on film. This method was used since the 1930s for the conservation, retransmission, and sale of television programs before the introduction of the videotape. The frame rate most used by this machine, since its origins, was 24 fps (cinema format). In the 1970s, however, hand in hand with the diffusion of colour TV, kinescopes capable of filming at 29.97 fps (NTSC standard) were introduced. [25] The digital images that were the subject of this study, provided by Mark Gray of the SPACECRAFT FILMS company (Atlanta GA), present all the 29.97 fps that were produced by the Scan Converter RCA: this is proven by the exact succession of

[25] *Frederick M. Remley, Magnetic Recording: The First Hundred Years (1998) New York, IEEE Press*

the dominant colours on the contours of the moving objects.[26] This allows us to say that the analysed material is complete and authentic, i.e. there are no cloned frames typical of 24/30 fps conversions, nor have new frames been generated by means of digital interpolation processes. The transition from analogic images to digital images has certainly led to a change in the aspect ratio which must be taken into account if we want to correctly interpret the position of the objects in each frame.

A.3.4.1 Display Aspect Ratio

The term *Display Aspect Ratio* (DAR) indicates the mathematical relationship between the width and height of an image. As we saw in A.2.1.2 the CTV sensor had dimensions 12,8 x 9,6 mm (Aspect Ratio 4:3 or 1,33). The television broadcast produced 525 TV lines in the NTSC format maintaining a DAR of 1,33. The images were subsequently impressed on film by the Kinescope with 10,26 x 7,49 mm format: the ratio between the two dimensions is 1,37.
Finally, the digital images contained by the Spacecraft Film DVDs have a size of 720x480 pixels in the 4:3 DVD -Video NTSC format. By starting from these data to understand how to find the correct proportion between the two frame sizes, it is necessary to make some considerations.

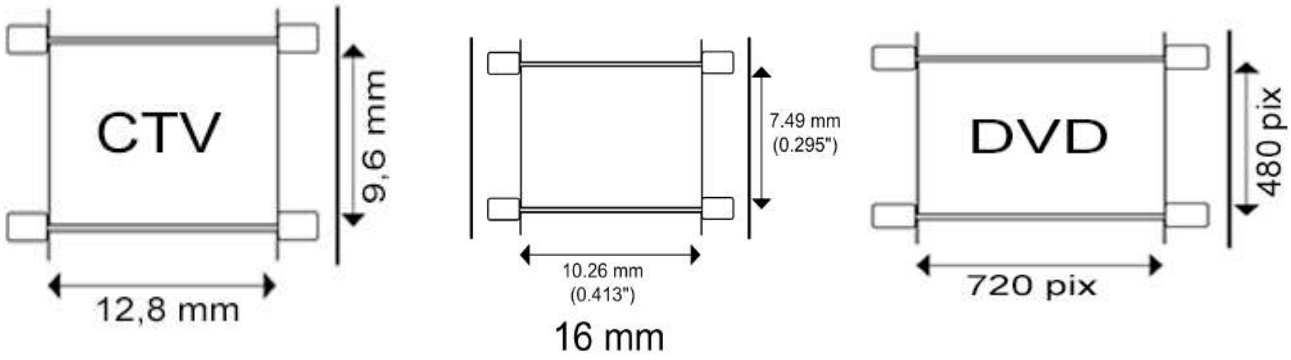

Figure A18 – Display Aspect Ratio changes undergone by CTV images during the main conversions

The resolution problems in the conversion of an analogic image into digital, have been the subject of a recommendation by the International Telecommunication Union known as Rec. 601, BT. 601 or CCIR 601, which actually defined the standard in 1982 [27]. Since then, analogic video signals have been sampled at 13.5 MHz. The number of active video pixels per TV line is equal to the sampling frequency multiplied by the duration of the active line (the part of each analogic video line that contains active video, thus not containing synchronization pulses, black bands, etc.). In the NTSC signal with 525 lines at 60 Hz, the duration of the active line is 52.856 µs and gives rise to ≈ 713.5 pixels per line. In order to avoid cutting parts of the active image, if the timing of the analogic video was equal to or greater than the tolerances established in the relevant standards, a total length of the digital line of 720 pixels was chosen.

---

[26] *For example, in image 25 the astronaut profile to the right of the frame presents the succession of colours frame x: RED; frame x+1: GREEN; frame x+2: BLUE which correspond to the colour of the last field superimposed by the RCA Scan Converter on earth. On the opposite profile, to the left of the frame, the astronaut presents a sequence CYAN (blue+green), YELLOW (green+red), MAGENTA (red+blue) due to the tendency of the original succession of colours (red+blue+green) to mix with each other when the motion is perceived by the machine as slower.*

[27] *https://www.itu.int/dms_pubrec/itu-r/rec/bt/R-REC-BT.601-7-201103-I!!PDF-E.pdf: Studio encoding parameters of digital television for standard 4:3 and wide screen 16:9 aspect ratios, Recommendation ITU-R BT.601-7 (03/2011). International Telecommunication Union Electronic Publication, Radiocommunication Sector, Geneva 2017* [Ann. 5]

But the active lines in the NTSC television format are only 483 (a value that is approximated to 480), so, in order to contain the alteration of the proportion, the digital product has thin black bars (8 pixels) to the right and left of the image and reproduces the analogic data in 704 pixels. The images provided by Spacecraft Films are in fact images of 720 x 480 pixels with black bands of 8 pixels on each side (nominal analogue suppression).

A.3.4.2 Pixel Aspect Ratio

In digital video, and with particular reference to display devices, the *Pixel Aspect Ratio* (PAR) was introduced with the aim of identifying what is the relationship between the density of information reachable on the ordinate axis compared to that achievable on the abscissa axis. The LCD monitors used in modern computers have an intrinsic PAR of 1, that is, they display equally dense information on the two axes. The analogic television signal has a precise number of scan lines, but not a precise number of columns, thus making it unnecessary to introduce the PAR concept.

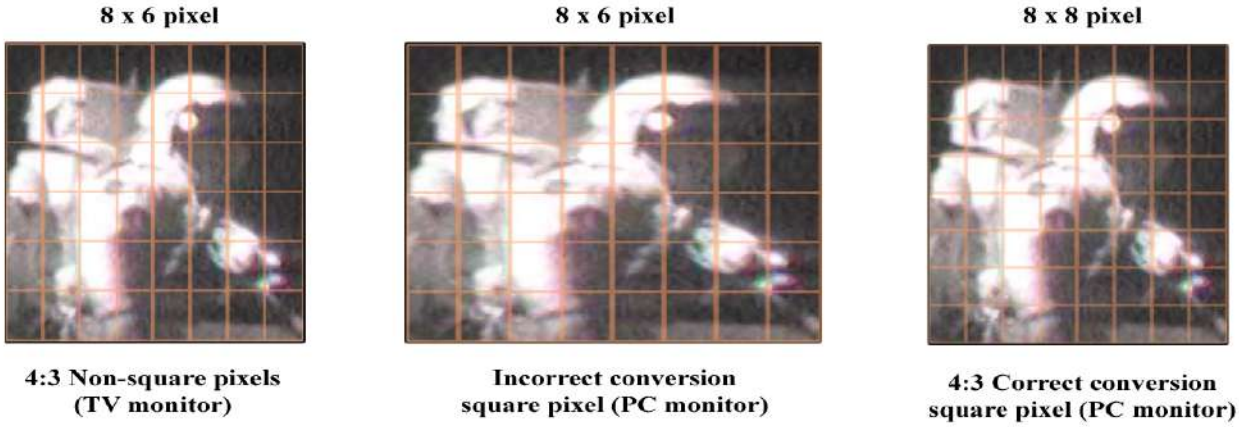

Figure A19 – Conversion from TV format to PC format

ITU-R BT.601 specified that the standard definition television images must be encoded by lines of 720 pixels (704 pixels of pure image) sampled at 13.5 MHz, but the encoding identifies non-square pixels. The analogic format NTSC, in fact, finds in the homologous digital format 704 x 480 pixels the preservation of the aspect ratio because the referred pixels have a PAR equal to 10/11. Having to view the images of the DVD-Video NTSC format with software operating on a square pixel system, this conversion coefficient must be taken into account [28]. The correct aspect ratio of the images on such a system will be obtained by bringing the image to 640x480 pixels.

A.3.5 Other possible alterations

We cannot be sure of how many successive conversions and transformations the lunar shoots have undergone after the already heavy production process, before reaching us in the form delivered by Spacecraft Films. However, it is certain that, as confirmed in all the cases that we will present below from the findings made on the known dimensions, the dimensional proportions are correct. Apollo mission researchers also agree that the videos distributed by Spacecraft are reliable sources, perhaps the best reproductions of the original films ever authorized by NASA.

---

[28] https://helpx.adobe.com/uk/photoshop/using/creating-images-video.html *Adobe Photoshop User Guide, Video and animation, Creating images for video © 2019 Adobe 345 Park Avenue S. Jose, CA 95110-2704*

Our analyses seem to confirm that no particular artefacts or filters have been introduced for the production. Proof above all, the very accentuated phenomenon of the flickering of the colours that we have exposed in paragraph A.3.2: any hypothetical restoration intervention that did not have a conservative character, and that tried to attenuate this effect, very annoying for the viewer, would have made the sequence of colours emerging on the contours of the moving objects less evident, or even completely altered the order of the dominant colours.

A.3.6 Preparation of videos for the correct metric measurements

Before proceeding to measurements with specific instruments, it was decided to prepare the films to be analysed with a software that represents the professional standard for video editing: Adobe Premiere CS6 [29]. The preliminary operations carried out were in summary:

1) Correction of the aspect ratio of the movie according to the good practices described in A.3.4.1 and A.3.4.2
2) Correction of geometric distortions considering what has been identified in A.2.2

Here below we describe the operations performed to obtain the corrections referred to in points 1 and 2, in order to favour repeatability (the same results can be achieved by using procedures and software able to guarantee the same quality of work):

a) Import the movie that interests us (for example .VOB files of Spacecraft Film DVD) in 720x480 format
b) Following a specific software request, at the end of the import procedure, to adjust the sequence settings to the video
c) Isolate the frames that interest us with the Adobe Premiere editing tools
d) Through its Effects panel choose the transform section, then apply the "crop" tool to the movie, cutting out the image and thus excluding any black band or outline
e) Export the movie by choosing the Mpeg2 format
f) In the panel "export settings / movie output tab" select "scale to fill"
g) In the basic video settings, choose the following parameters: 640x480 format; square pixels (1,000); fps 29.97; level: high; bitrate: VBR 2 passages, maximum depth (put the 3 sliders to the 80 value); maximum rendering quality.
h) Confirm the export settings and then save the new movie.

Saving in MPEG2 format is necessary for the analysis described below in A.4, using the Tracker Video Modeling software. Another procedure that we report, more complex but from which a better result is obtained, is the export from Adobe Premiere in TIFF format. Also in this case we recommend selecting the 640x480 square pixel format and proceeding to export with the highest quality and depth of Rendering. The TIFF format is an uncompressed format and retains all the original data, thus allowing a more accurate measurement. In case of analysis with Adobe Photoshop or other similar editors, all TIFF images must be loaded on different levels in the same work area, so that the same measurement system can be applied. For measurements with other software that allows tracking only on video files (e.g. Tracker Video Modeling), in case the quality result of the conversion from the VOB format is poor, in order to maintain the high quality of the source it is possible:

---

[29] https://helpx.adobe.com/it/premiere-pro/user-guide.html *Adobe Premiere Pro User Guide, © 2019 Adobe 345 Park Avenue S. Jose, CA 95110-2704*

1) To export movies from VOB to TIFF with Adobe Premiere [*Ann. A8*]
2) To transform TIFF files in MP4 sequence (compatible with Tracker Video Modeling) through the option of Adobe Photoshop: Open / Sequence of Images and then Export / Rendering Video [*Ann. A9*]

A.4 ANALYSIS WITH TRACKER VIDEO MODELING [*Ann. A10*]

Tracker [30] is a free video analysis and modeling tool very well known by teachers and students all over the world. It's built on the Open Source Physics (OSP) Java framework [31], completely free and open source. It is designed to be used in physics education. It collected over 1 million users in 26 different languages. Tracker video modeling is a powerful way to combine videos with computer modeling. (The authors: Douglas Brown, Wolfgang Christian, Robert M. Hanson)

Tracker Video Modeling (TVM) is a very useful tool for tracking kinematic models starting from digital images and movies. Its features allow you to track moving objects, and obtain metric data, speeds, and accelerations in a very agile way. It is possible to create models of material points and masses, as well as multi-body systems. It makes use of interactive vector graphics and has very interesting analysis tools such as the Autofit, capable of estimating the best theoretical model for each track identified. Although it also implements a perspective straightening function, measurements, and calibrations on TVM are possible on a single plane only. This means that it is not possible to solve the three-dimensional space and make scientifically reliable measurements when the objects that allow the calibration of the system are on planes different than the measurement one. However, for the sequence under study in this section, the software is efficacious, considering that the motion that we will try to trace can be detected starting from the same object with which we can calibrate the system.

A.4.1 Set up of measurement system.

The first operations to be carried out for the correct use of the software are:

1) Perspective straightening and system Calibration through the enhancement of height and width of the OPS Unity (66,04 cm X 48,26 cm) *(Menu - Tracks - New - Calibration tool; subsequently with Video - Filters - New - Perspective to obtain the balance of the two measures: see the values presented in figures A21 and A22)*

2) Appropriate positioning of the Cartesian axes X, and Y and therefore of the origin of the measurement system *(Menu - Tracks - Axes)*

---

[30] https://physlets.org/tracker/ Tracker, Video Analysis and Modeling Tool, Copyright 2019 Douglas Brown, GNU General Public License, Version 3.

[31] http://www.opensourcephysics.org/ © 2003-2020 AAPT-ComPADRE National Science Digital Library. Managing Editor: Wolfgang Christian - Davidson College (USA); Developers: Doug Brown - Cabrillo College, Francisco Esquembre - Universidad de Murcia (ES).

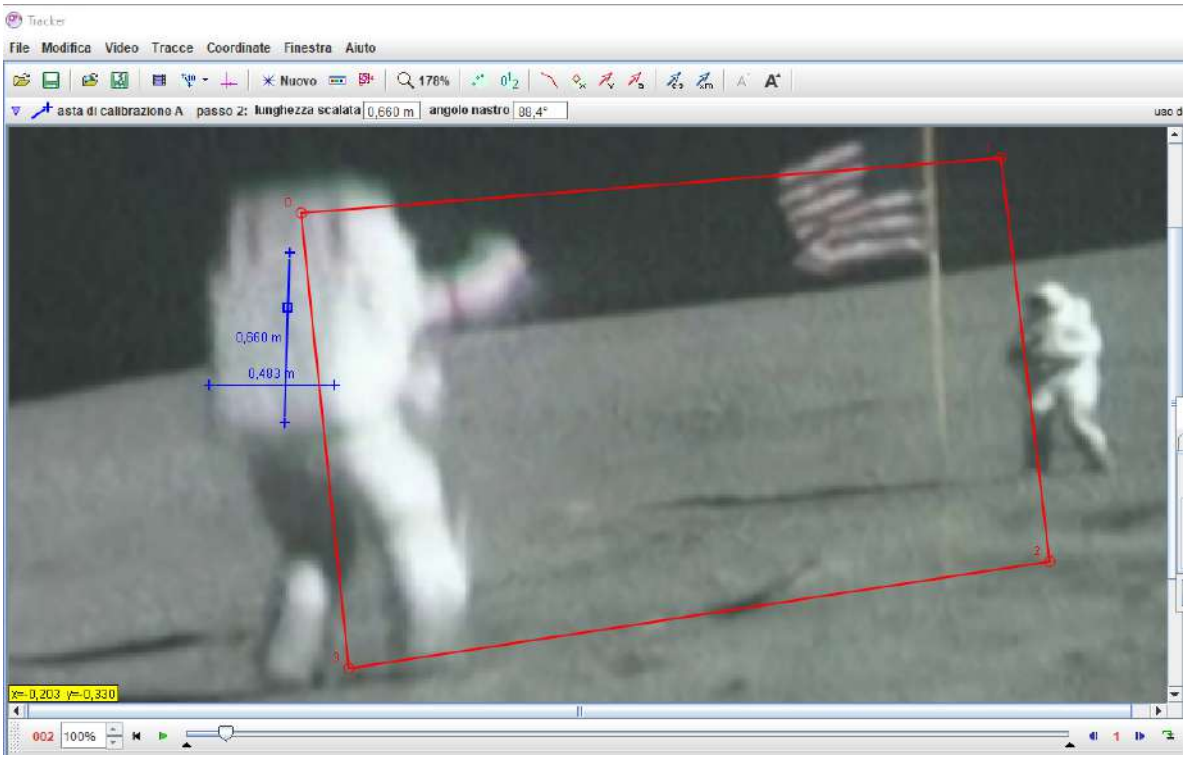

Figure A20 – Perspective straightening with Tracker Video Modeling

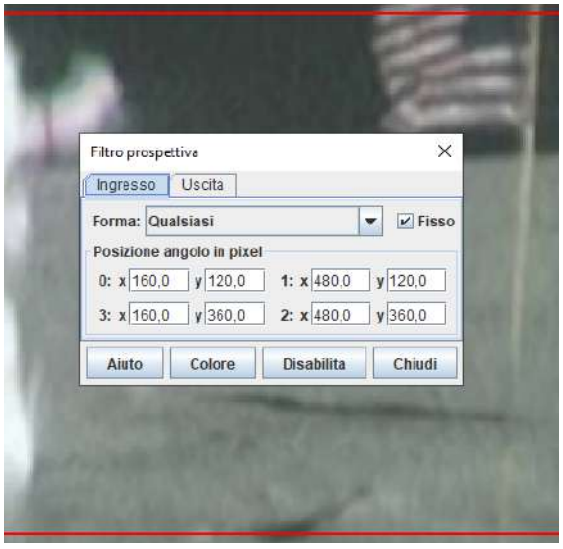

Figure A21 – Tracker: input straightening values

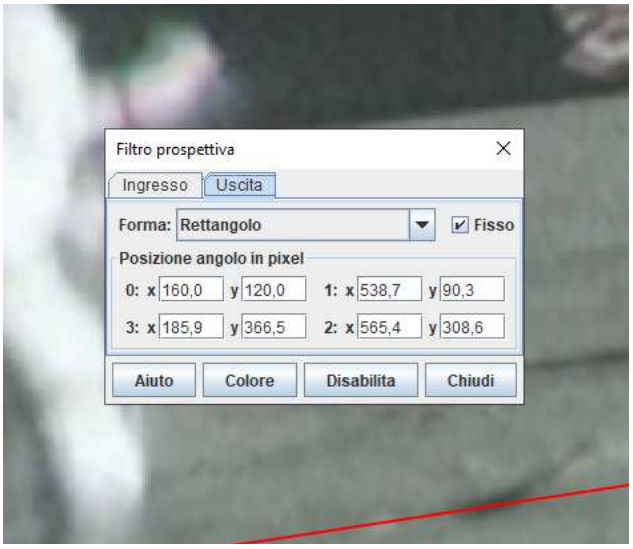

Figure A22 – Tracker: output straightening values

With the "Point of Mass" tool (Menu - Tracks - New - Point of Mass) it is now possible to proceed with the detection of the quotas that a point suitably chosen on the PLSS Unity reaches progressively in each of the frames of the sequence, during each of the two jumps by John Young (below we present the analysis and the results relating to **the second jump of the astronaut**, the procedure can be repeated for the first jump with analogous results).

A.4.2 Detection results. [*Ann. A11*]
Table A2 shows the quotes in meters on the Y-Axis (height), reached by the upper edge of the OPS module that John Young carried on his shoulders during the jump. They were identified with TVM with respect to the Cartesian system adopted, and refer to the 45 frames of the sequence recorded by the CTV. In the last column you can compare the values obtained with those of a model built according to the hourly law:

$$Y_{mod} = Y_0 + (Vy_0 * t) - (\tfrac{1}{2} * g * t^2)$$

setting in the equation Vy0 = 1,05 m / s as suggested by Eric M. Jones in the Apollo 16 Lunar Surface Journal released by NASA. As you can see, the model proposed by NASA is not the best model to interpret the tracked motion. The TVM software, through the "Autofit" function, available in the "Analysis" section *(Window - Analysis - Select t horizontal and Y vertical columns - Flag on Autofit)* identifies the following as the most appropriate values for the 3 independent variables of the equation:

Y_0 = 1,907E-2 m
Vy_0 = 1,225 m/s
1/2g = -8,442E-1 m/s^2

In particular, the lunar g results to be 1,69 m/s^2: this is a surprisingly accurate estimate of the well-known value 1,62 m/s^2. In constructing the "Tracker" model, we will take into account only the initial speed calculated by the software, keeping the known values for Y_0 and g. In the model proposed by Eric M. Jones, Astronaut Young would touch the ground approximately 1,30 seconds after the jump, while from the measurements it would seem that this event should be recorded between frame 43 and frame 44, thus between 4/30 and 5/30 of a second later. To compare the two models and decide which is actually the best, we rely on the statistical test of CHI SQUARE.

χ^2(Y, Ytracker) = 9,999*10^{-1}
χ^2(Y, Ynasa) = 4,171*10^{-45}

Frame	Time	Y	$Y_{tracker}$	Y_{nasa}
0	0,00E+00	0,00E+00	0,00E+00	0,00E+00
1	3,34E-02	4,81E-02	3,98E-02	3,41E-02
2	6,67E-02	9,53E-02	7,78E-02	6,65E-02
3	1,00E-01	1,37E-01	1,14E-01	9,70E-02
4	1,33E-01	1,76E-01	1,48E-01	1,26E-01
5	1,67E-01	2,09E-01	1,81E-01	1,53E-01
6	2,00E-01	2,39E-01	2,12E-01	1,78E-01
7	2,34E-01	2,68E-01	2,41E-01	2,01E-01
8	2,67E-01	2,95E-01	2,68E-01	2,23E-01
9	3,00E-01	3,15E-01	2,93E-01	2,42E-01
10	3,34E-01	3,35E-01	3,17E-01	2,60E-01
11	3,67E-01	3,54E-01	3,39E-01	2,76E-01
12	4,00E-01	3,71E-01	3,59E-01	2,91E-01
13	4,34E-01	3,88E-01	3,77E-01	3,03E-01
14	4,67E-01	4,05E-01	3,93E-01	3,14E-01
15	5,01E-01	4,18E-01	4,08E-01	3,23E-01
16	5,34E-01	4,31E-01	4,20E-01	3,30E-01
17	5,67E-01	4,42E-01	4,31E-01	3,35E-01
18	6,01E-01	4,50E-01	4,41E-01	3,38E-01
19	6,34E-01	4,55E-01	4,48E-01	3,40E-01
20	6,67E-01	4,60E-01	4,53E-01	3,40E-01
21	7,01E-01	4,63E-01	4,57E-01	3,38E-01
22	7,34E-01	4,65E-01	4,59E-01	3,34E-01
23	7,67E-01	4,63E-01	4,59E-01	3,29E-01
24	8,01E-01	4,61E-01	4,58E-01	3,21E-01
25	8,34E-01	4,55E-01	4,54E-01	3,12E-01
26	8,68E-01	4,49E-01	4,49E-01	3,01E-01
27	9,01E-01	4,40E-01	4,42E-01	2,89E-01
28	9,34E-01	4,28E-01	4,33E-01	2,74E-01
29	9,68E-01	4,15E-01	4,22E-01	2,58E-01
30	1,00E+00	4,00E-01	4,10E-01	2,39E-01
31	1,03E+00	3,81E-01	3,95E-01	2,19E-01
32	1,07E+00	3,62E-01	3,79E-01	1,98E-01
33	1,10E+00	3,42E-01	3,61E-01	1,74E-01
34	1,13E+00	3,19E-01	3,42E-01	1,49E-01
35	1,17E+00	2,94E-01	3,20E-01	1,22E-01
36	1,20E+00	2,68E-01	2,97E-01	9,25E-02
37	1,23E+00	2,40E-01	2,72E-01	6,17E-02
38	1,27E+00	2,12E-01	2,45E-01	2,91E-02
39	1,30E+00	1,84E-01	2,16E-01	-5,28E-03
40	1,33E+00	1,54E-01	1,85E-01	-4,15E-02
41	1,37E+00	1,19E-01	1,53E-01	-7,95E-02
42	1,40E+00	8,44E-02	1,19E-01	-1,19E-01
43	1,43E+00	4,53E-02	8,30E-02	-1,61E-01
44	1,47E+00	-2,09E-05	4,52E-02	-2,04E-01
45	1,50E+00		5,68E-03	

Table A2 – Big Navy Salute: quote Y, comparison of theoretical models (apex and extreme of traced motion in yellow)

The test was carried out on the measurements in centimetres, excluding the comparison values lower than 5 units, giving 35 degrees of freedom for each of the two checks: set the significance index α = 0,05 (p-value 49,80), note that the model proposed by "Tracker" passes the test while that one proposed by NASA definitely does not.

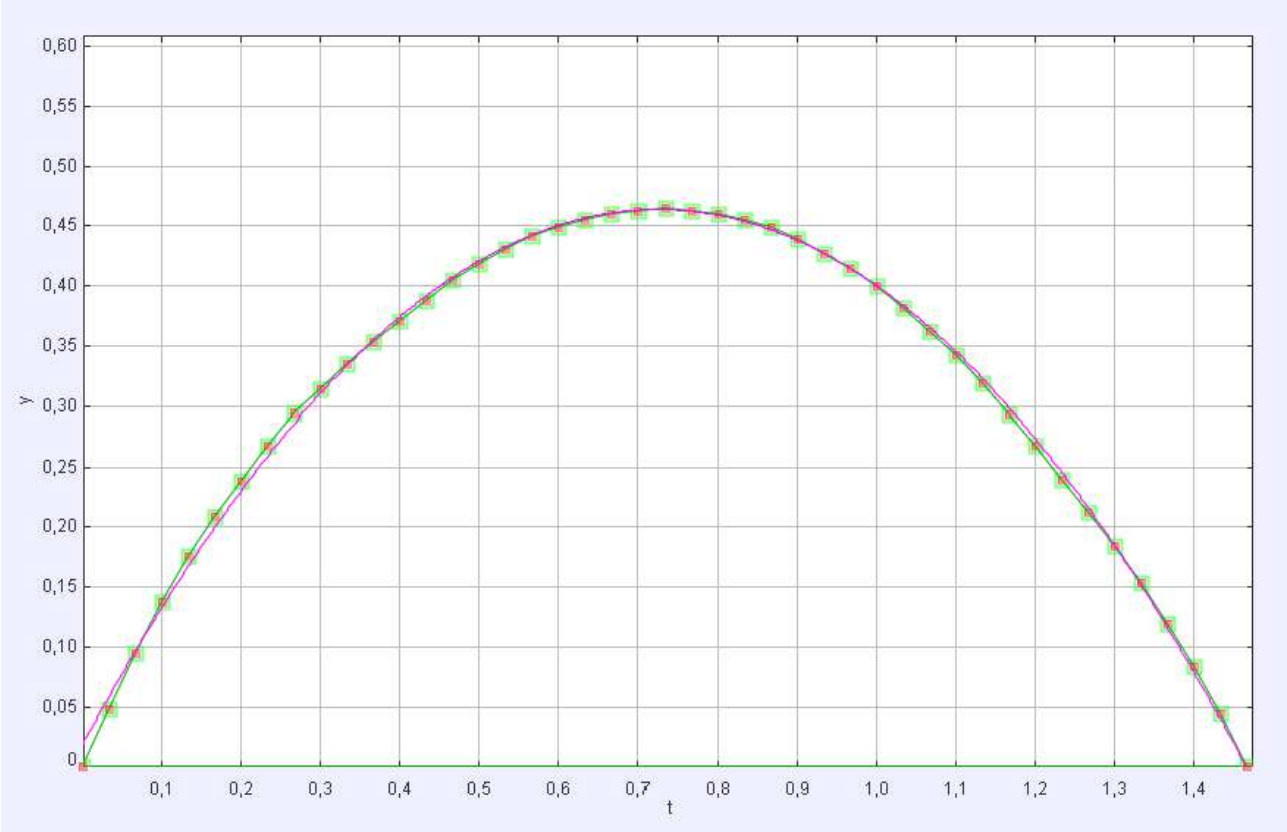

Figure A23 – Motion plot compared with the Autofit curve (red) generated by Tracker Video Modeling

A.4.3 Analysis of the Experimental Error

Similarly to the measurements made with Photoshop CS6 in C.3.7, also for TVM the instrumental error can be referred to as the unit of measurement in pixels. Considering that also on this software we proceed with the same system calibration operations and point positioning, the overall error is equivalent to +/- 1,5 pixels, which is, in the specific context, +/- 1 cm in reality. For most of the track, the maximum differences between the Tracker model and the experimental values are maintained within this confidence interval, thus confirming the validity of this theoretical model. This cannot be said for the model proposed by NASA on Lunar Surface Journal.

SECTION B
61135 Falls So Slowly

Figure B1 – Station 1, 4° sample site. Young's shadow is at the right and Flag Crater is in the background. [32]

B.1.1 EVA 1 [33]

The first extravehicular activity of Apollo 16, as we have seen, was characterized by the installation of equipment for scientific experimentation, an operation carried out, as always, within a short radius of the landing site. Once this phase was concluded, again within the context of EVA 1, the

[32] https://www.hq.nasa.gov/wp-content/uploads/static/history/alsj/a16/AS16-109-17799HR.jpg *Apollo Image Library, Apollo 16 Figure Captions Copyright © 1996-2017 by Eric M. Jones, last revised 16 March 2019.*

[33] https://www.hq.nasa.gov/wp-content/uploads/static/history/alsj/a16/a16.html *Apollo 16 Lunar Surface Journal Corrected Transcript and Commentary by Eric M. Jones. Revised 5 March 2016.*

first short trip with the Lunar Rover (LR) was made, towards the Plum, Flag, and Ray craters. The EVA lasted 7 hours and 11 minutes in total. The distance travelled was 4,2 km. Station 1 was located about 1400 meters west of the LM near the edge of the Plum Crater. The astronauts collected samples, and took panoramic and stereographic photos.

B.1.2 DESCRIPTION OF SEQUENCE [2]

123:46:09 *Young: How we doing on time, Tony?*
123:46:10 *England: Okay, you've got about 23 minutes left, here.*
123:46:15 *Duke: Twenty-three! Hum.*
123:46:19 *England: Rog.*
123:46:21 *Duke: By golly. We can pick up a lot of rocks in 23...Hey, I'd like to go to the other side, John, of Plum because those rocks over there aren't dust covered, if you can see them.*
123:46:32 *Young: That's a good idea, Charlie.*
123:46:34 *Duke: See right out there towards South Ray?*
123:46:36 *Young: Yeah.*
123:46:37 *Duke: Those rocks don't look as dust covered as these. (Pause)*
[Charlie gets into position with his back to us and slides the scoop under a fist-sized rock next to the up-Sun gnomon leg. As he raises the rock, it starts to fall out of the scoop.]
123:46:48 Duke: Uh-oh. Agh. I missed. Wait a minute.
[Because things fall so slowly on the Moon, Charlie is able to bat the rock upward repeatedly as he chases it to his right. It finally falls to the ground.]
123:46:53 *England: Nice juggling!*
123:46:56 *Duke: Well, it wasn't dust covered. (Responding to Tony) Well, we missed it. But things really fly up here. I'm amazed.*
[Charlie gets the rock in the scoop and raises it high enough that John can grab it. John shakes his hand to try to get some of the dust off. This is sample 61135, a 0,25 kg breccia.]

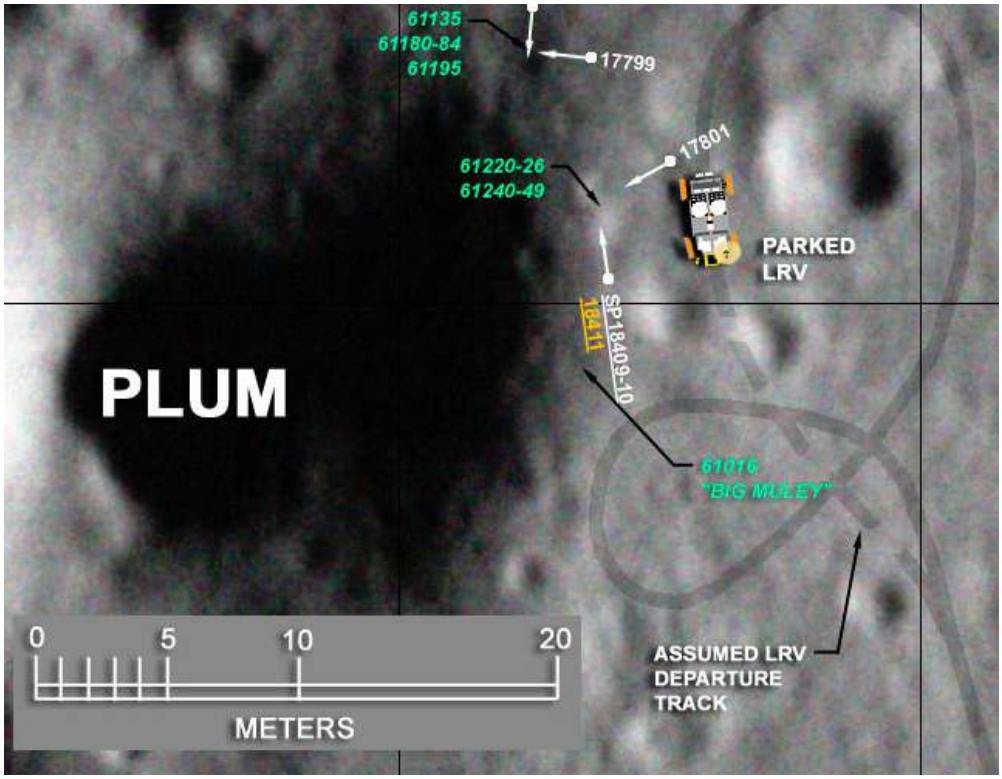

Figure B2 – Extract of the planimetric map of the STATION 1, EVA 1 of Apollo 16, produced by Brian McInall [3]

B.1.2.1 Sources: The images used for this study are taken from Apollo 16 Journey to Descartes, complete TV and onboard film © 2005 Spacecraft Film (courtesy NASA). The sequence relating to the collection of sample 61135 is published at this link: https://youtu.be/8Tgej1RmeWs [*Ann. B1*]

B.1.2.2 Other official sources containing the same sequence:
- Apollo 16 Lunar Surface Journal Corrected Transcript and Commentary by Eric M. Jones 1996, *Revised 24 April 2017.*
https://www.hq.nasa.gov/wp-content/uploads/static/history/alsj/a16/a16v.1234609.mpg

B.1.2.3 The free-fall rock sample [35]
Sample 61135 collected during EVA 1 at the fourth site of STATION 1 is an ancient breccia of regolith of 245,1 gr, which compacted around 3,9 billion years ago. Due to the exposure to cosmic rays lasting about 50 million years, it has several microcraters. It is a clastic breccia made up of many components. The geological studies that concern it are not concordant at the moment (probably because they have concentrated on different portions). The lithic fragments include basalt, granoblastic anorthosite, and noritic rock. It contains a high glass percentage but few recognized agglutinates.

Figure B3, Apollo 16, Lunar Finding 61135

B.2 ABERRATION OF IMAGES
With the same procedure followed in A.2.1.1 and A.2.1.2, we use the available floor plan (see figure B2) to derive the distance of the scene from the objective. According to the data processed by Brian McInall, on the basis of the information made available by NASA, the sequence takes place at about 10 m from the objective. Using the same formula shown in A.2.1.2:

$$F = OY \cdot \frac{PLSS_{ctv}}{PLSS_r}$$

with $PLSS_{ctv}$ = 2,2 mm, $PLSS_r$ = 660 mm, and 1 px as the instrumental error we find:

F = 33,33 mm (+/- 1,6 mm)

---

[34] *https://www.hq.nasa.gov/wp-content/uploads/static/history/alsj/a16/A16_EVA_1_STA_1_Planimetric_Map-LROC_M177535538L_Feb_2018.jpg Apollo 16 Lunar Surface Journal Corrected Transcript and Commentary by Eric M. Jones. Revised 5 March 2016.*

[35] *https://curator.jsc.nasa.gov/lunar/lsc/61135.pdf 61135 Lunar Sample Compendium C. Meyer 2009* [*Ann. B2*]

The equivalent focal length compared to the standard format 35 mm is:

$Fe = F \cdot \frac{D_S}{D}$ = 33,33 x 43,3 / 16 = 90 mm (+/- 4 mm)

Considering the typical distortion of the CTV of 2% and a distortion due to the focal length between 86 and 94 mm (light telephoto) it is appropriate to adopt a percentage of geometric distortion higher than 2% and less than 3% (maximum declared). The choice goes on the value 2,5% as a percentage of positive distortion (pincushion) to be corrected on the images of the sequence.

B.3.1 ANALYSIS WITH TRACKER VIDEO MODELING

By proceeding as already illustrated in A.3.6 and A.4.1 we adopt the best procedures for the preparation of the films and the measurement system, taking care to scale the images [*Ann. B3*] considering the Aspect Ratio, the Pixel Aspect Ratio, following the good practices for the digital video conversion [*Ann. B4*] and implementing the geometric aberration correction produced by the CTV optical group according to the value just calculated in B.2.

The frames that strictly concern the free-fall motion of sample 61135 are 40 (of which the first 12 show an upward motion of the breccia), and at 29.97 fps indicate an overall duration of the sequence of 1,30 s. With TVM, having identified the plane on which the motion insists, we perform the perspective straightening as shown in figures B4-B5-B6.

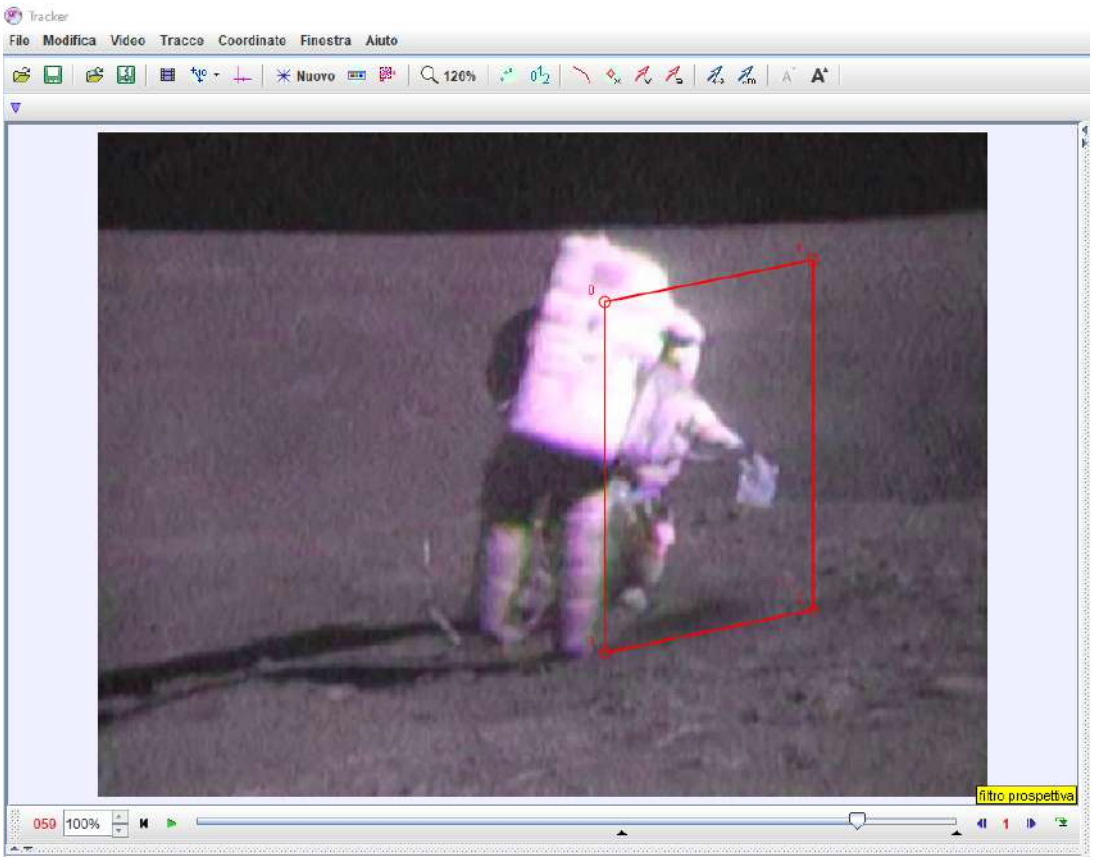

Figure B4 – Perspective straightening with Tracker Video Modeling

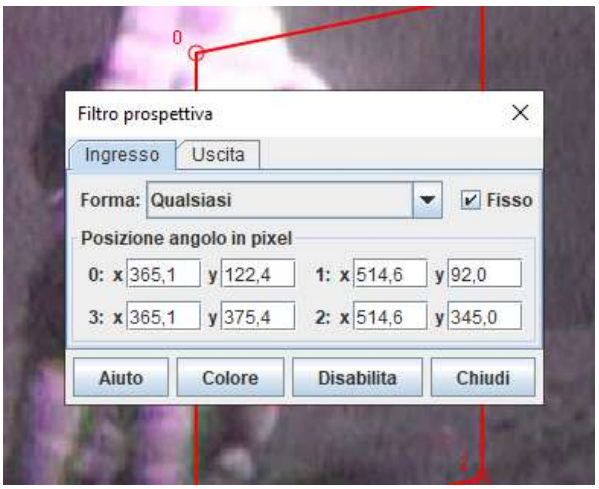

Figure B5 – Tracker: input straightening values

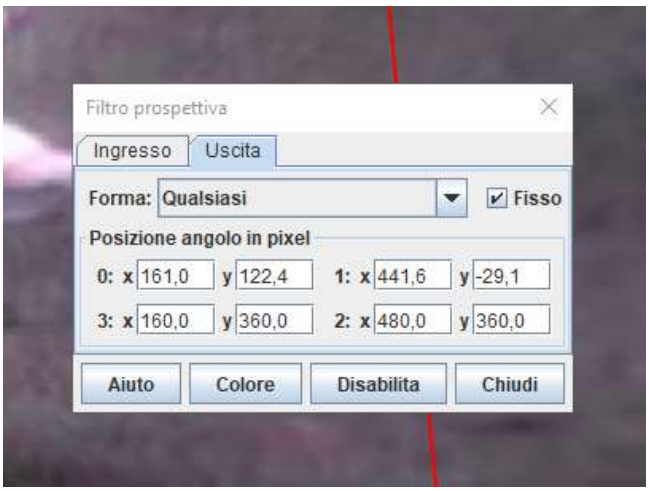

Figure B6 – Tracker: output straightening values

At this point, we set the Cartesian plane X, Y with origin in a conventional point (in our case near the base of the right heel of Charlie Duke), and through the tool "Point of Mass" we proceed to trace the centre of the breccia of regolith in the 40 frames that immortalize the last stages of its ascent and its definitive fall towards the ground. In 8 frames the identification of the body position is impossible. In particular, between frames 25 and 30 the breach is covered by the Sample Bag that John Young is holding in his hand. [*Ann. B5*]

B.3.2 Results of detecting. [*Ann. B6*]

Table B1 shows the results obtained. The hourly model of comparison can be indicated with the equation: $y = y_0 + (V_{y_0} \cdot t) - (\frac{1}{2} \cdot g \cdot t^2)$

The curve is fitted from the data collected using the TVM Autofit tool.

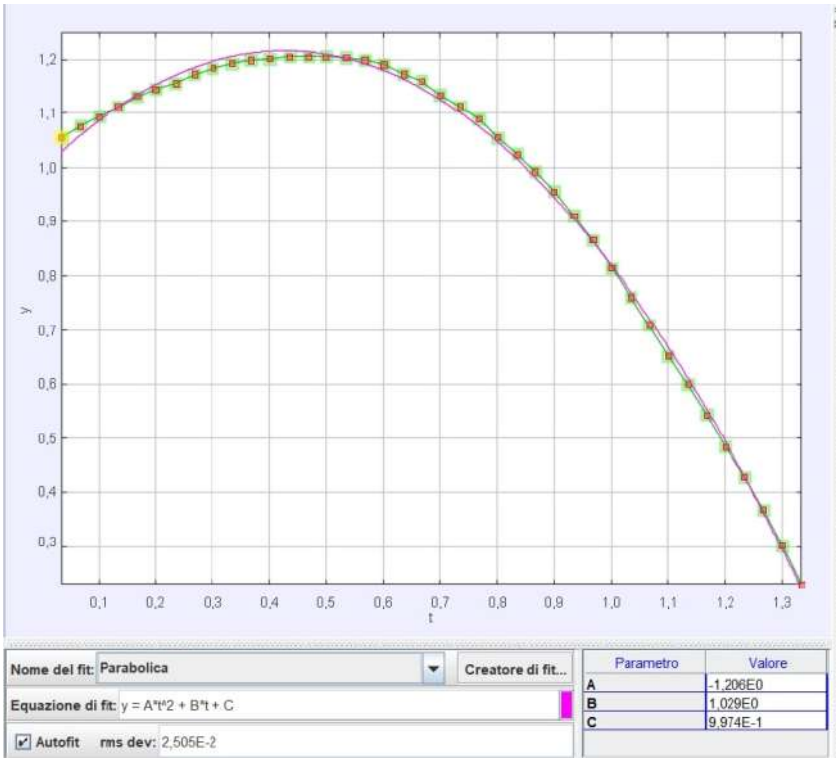

Figure B7 - Motion plot (green) compared with the Autofit curve (red) proposed by Tracker Video Modeling

The software derives $\frac{1}{2}\, g_{tvm} = -1.201 \pm 0{,}011\ m/s^2$ from which

$g_{tvm} = (-2{,}40 \pm 0{,}022)\ m/s^2$

The inconsistency with the expected g value (g = - 1.62 m/s^2) forces us to seek confirmation of the measurements obtained. Photoshop CS6 is then used to examine the same sequence.

B.3.3 ANALYSIS WITH PHOTOSHOP CS6

Similarly to what has been put into practice in the previous sections, we use the Adobe Photoshop CS6 Vanishing Point Filter to "solve" the spatial model of the environment in which the sequence takes place, in order to correctly identify the measurement plane and the right system of coordinates that allow us to trace the fall of the breccia 61135. [*Ann. B7*]

The relevant known dimensions are many:

- the dimensions of the PLSS already acquired in A.2.1.1.1:
PLSS height: m 0,6604
PLSS width: m 0,4826

- the length of the Large Adjustable-angle Scoop and of the relative pan (figure B8) [36]:
Scoop length: 0,91 m
Pan length: 0,152 m

- the height of the Lunar Sample Bag, which however resides on a more advanced plane than the measurement one (for the confirmation of this data, please refer to D.2.1)
Lunar Sample Bag height: 0,21 m

With these references, the plane on which it is possible to trace the motion of the breccia can be approximated to that in figure B9.

Frames	T (s)	Y (m)	Y_{tvm} (m)
0	0,000	1,055	0,997
1	0,033	1,077	1,030
2	0,067	1,095	1,060
3	0,100	1,113	1,088
4	0,133	1,132	1,113
5	0,167	1,146	1,135
6	0,200	1,157	1,155
7	0,234	-	1,172
8	0,267	-	1,186
9	0,300	1,193	1,197
10	0,334	1,200	1,206
11	0,367	1,202	1,212
12	0,400	1,207	1,216
13	0,434	1,207	1,216
14	0,467	1,207	1,215
15	0,501	1,204	1,210
16	0,534	1,200	1,203
17	0,567	1,191	1,193
18	0,601	1,175	1,180
19	0,634	1,161	1,165
20	0,667	1,135	1,147
21	0,701	1,113	1,126
22	0,734	1,090	1,102
23	0,767	1,056	1,076
24	0,801	1,025	1,048
25	0,834	-	1,016
26	0,868	-	0,982
27	0,901	-	0,945
28	0,934	-	0,906
29	0,968	-	0,863
30	1,001	-	0,819
31	1,034	0,709	0,771
32	1,068	0,652	0,721
33	1,101	0,601	0,668
34	1,134	0,544	0,612
35	1,168	0,484	0,554
36	1,201	0,429	0,493
37	1,235	0,368	0,429
38	1,268	0,303	0,363
39	1,301	0,230	0,294

Table B1 – Collection of sample 61135: Y quotas and comparison with the Y_{tvm}

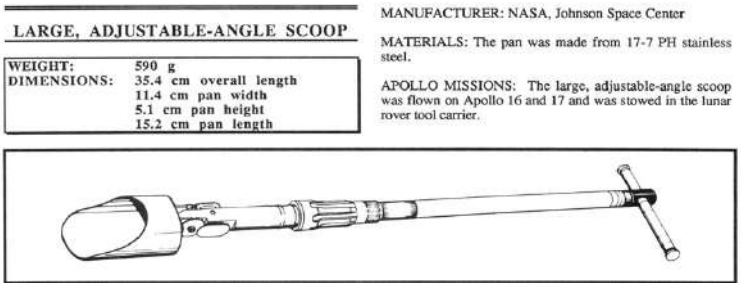

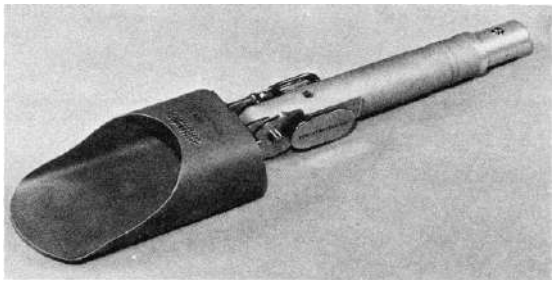

[36] https://curator.jsc.nasa.gov/lunar/catalogs/other/jsc23454toolcatalog.pdf - *Catalog of Apollo Lunar Surface Geological Sampling Tools – J. Haley Allton, Lockheed Engineering and Sciences Company, Houston (Texas) March 1989* [*Ann. B8*]

Figure B8 - Large Adjustable-angle Scoop

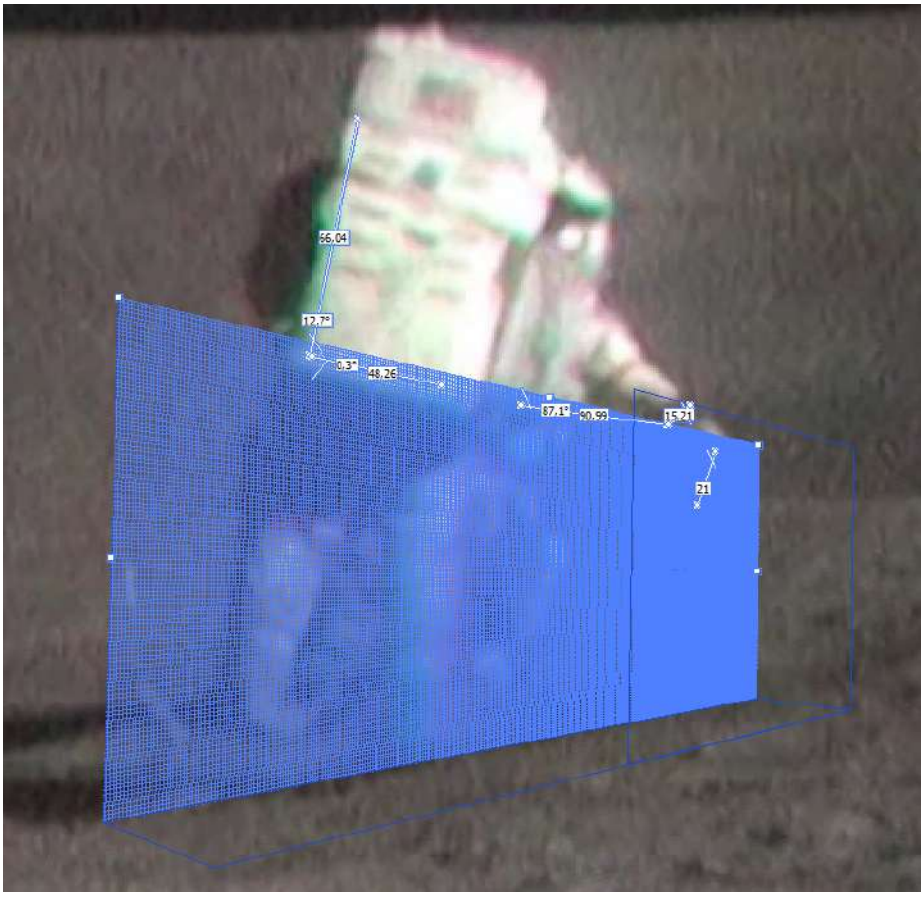

Figure B9 – Adobe Photoshop CS6 Identification of the measurement plan starting from known dimensions

The quotas of the breccia in the 40 frames included in the sequence are detected starting from the base of the plane in question with the exception of the 8 in which the breach itself is not identifiable [*Ann. B6*]. The results obtained are shown in table B2. In order to identify the best fit of the parabolic curve they express, the analysis is carried out with the professional software Origin Pro 2018.[37] [*Ann. B9*]

Equation z = Intercept + B1*t + B2*t^2

Parameters

		Value	Standard Error	t-Value	Prob>|t|
z	Intercept	1,02536	0,00374	274,07713	0
	B1	0,82477	0,01465	56,30735	0
	B2	-1,1134	0,01281	-86,93888	0

Standard Error was scaled with square root of reduced Chi-Sqr.
Some input data points are missing.

Statistics

	z
Number of Points	31
Degrees of Freedom	28
Residual Sum of Squares	10,95537
R-Square (COD)	0,99774
Adj. R-Square	0,99758

Summary

	Intercept		B1		B2		Statistics
	Value	Standard Error	Value	Standard Error	Value	Standard Error	Adj. R-Square
z	1,02536	0,00374	0,82477	0,01465	-1,1134	0,01281	0,99758

[37] *OriginLab at One Roundhouse Plaza, Northampton, MA 01060-4401 USA, http://www.originlab.com*

Figure B10 - Fit of the motion result with Origin Pro: parameters obtained and their reliability.

As can be seen from figure B10, the best estimation of the gravity acceleration acting on the sequence in question is $\frac{1}{2} g_{or} = -1{,}113 \pm 0{,}013\ m/s^2$ and so: $g_{or} = -2.22 \pm 0{,}026\ m/s^2$ (Standard Err). A relatively convergent value with the one obtained in the previous paragraph 3.2 and still largely inconsistent with the expected one considering that the scene was filmed on the Moon:

$$\frac{|g_{or} - g_m|}{\sigma} = \frac{|-2,22 + 1,62|}{0,026} = 23,08 > 3$$

B.3.4 Possible interpretation of the results

B.3.4.1 Systemic and accuracy errors

The first hypothesis that can be formulated in order to explain this inconsistency is that the instrumental error is not the only one causing the retrieval of experimental data so far from the elementary model of the applicable motion. Although in the previous case of study (section A), the measurements were immediately very reliable, it is necessary to list other possible sources of error as follows:

E1) Systemic errors in the sizing of the images and in the application of the geometric aberration caused by the lens

E2) Systemic errors in the correction of perspective distortion made by TVM

E3) Accuracy errors due to the quality of the images and their particular mechanism of production

With regard to E1, given that the preliminary sizing operations are analogous to those performed in the previous case study, based on the quality of the results achieved in that context, we can restrict the field to geometric aberration only. But in no way a percentage of distortion caused by the optical system, limited to 3% (technical limit declared by the manufacturers [38, 39]) can significantly affect the measurements made, since the motion takes place in a relatively central area of the image and any systemic errors of this entity, according

Frames	T (s)	Z (m)	Z_{or} (m)
0	0,000	1,038	1,025
1	0,033	1,065	1,052
2	0,067	1,083	1,076
3	0,100	1,102	1,097
4	0,133	1,116	1,116
5	0,167	1,127	1,132
6	0,200	1,14	1,146
7	0,234	-	1,157
8	0,267	-	1,166
9	0,300	1,168	1,172
10	0,334	1,173	1,176
11	0,367	1,176	1,178
12	0,400	1,17	1,176
13	0,434	1,172	1,173
14	0,467	1,164	1,167
15	0,501	1,157	1,158
16	0,534	1,153	1,147
17	0,567	1,139	1,134
18	0,601	1,123	1,118
19	0,634	1,11	1,099
20	0,667	1,091	1,078
21	0,701	1,068	1,055
22	0,734	1,043	1,029
23	0,767	1,016	1,000
24	0,801	0,979	0,970
25	0,834	-	0,936
26	0,868	-	0,900
27	0,901	-	0,862
28	0,934	-	0,821
29	0,968	-	0,778
30	1,001	-	0,732
31	1,034	0,665	0,684
32	1,068	0,615	0,633
33	1,101	0,564	0,580
34	1,134	0,515	0,524
35	1,168	0,464	0,466
36	1,201	0,412	0,406
37	1,235	0,35	0,343
38	1,268	0,286	0,277
39	1,301	0,214	0,209

Table B2 – Collection of sample 61135: $Z_{photoshop}$ quotas and comparison with the Z_{origin} model

[38] https://www.hq.nasa.gov/alsj/GCTA-Manual.pdf *RCA Government and Commercial Systems, Astro-Electronics Division, Princeton NJ 08540; Issued 24 May 1971, Revised January 1972 [Ann. 13]*

[39] https://archive.org/details/RcaUltriconSitCameraTubes *RCA-Norbain Electro – Optics Ltd. Seminar Electro – Optics/Laser International '82 UK Brighton 23-25 March 1982*

to the Brown-Conrady model [40], are certainly negligible unless they affect the edges of the image itself. Therefore, it seems possible to discard the first range of systemic errors defined in E1 as causes of the inconsistency between results and the expected model.

We can also discard E2, given the relative convergence of the results obtained with TVM and PS CS6. Finally, with regard to E3, we can estimate the highest uncertainty due to the superposition of 4 sequential fields joined in the same frame (see A.3.2): this could entail a (theoretical) difficulty in identifying the central point of the body to be traced, even if a clearer area of the breccia is actually always clearly visible in each frame, and moreover, the knowledge of the sequence of colours that characterize each half-field within the same frame, constitutes an excellent reference element in the detection of the perimeter and the centre of the body in each image.

In any case, considering the scheme shown in table A1, if we admit an uncertainty on the positioning of the material point caused by its possible belonging to one of the 4 fields of the same frame, it means we declare a theoretical error equivalent to:

$Err = z_x - z_{x+1}$; $\qquad Z_{Err} = \pm \frac{(z_x - z_{x+1})}{2}$

In the *Annex. B6* we report for each frame the experimental and accuracy errors quadrature-sum, both for the results obtained with TVM and with those obtained with PS CS6.

We deduce that the overlap of sequential fields recorded by CTV in order to convert the footage to the NTSC standard cannot determine an uncertainty that justifies the inconsistency found between the data and the reference model.

Let's exemplify everything with a graph obtained with the Origin Pro 2018 software in which the vertical segments that insist on the 32 detected points represent the maximum error that can be considered.

[40] *Duane C. Brown. "Decentering distortion of lenses",Photogrammetric Engineering, 32(3):444-462, 1966. Conrady, Alexander Eugen. "Decentred Lens-Systems." Monthly notices of the Royal Astronomical Society 79 (1919): 384–390.*

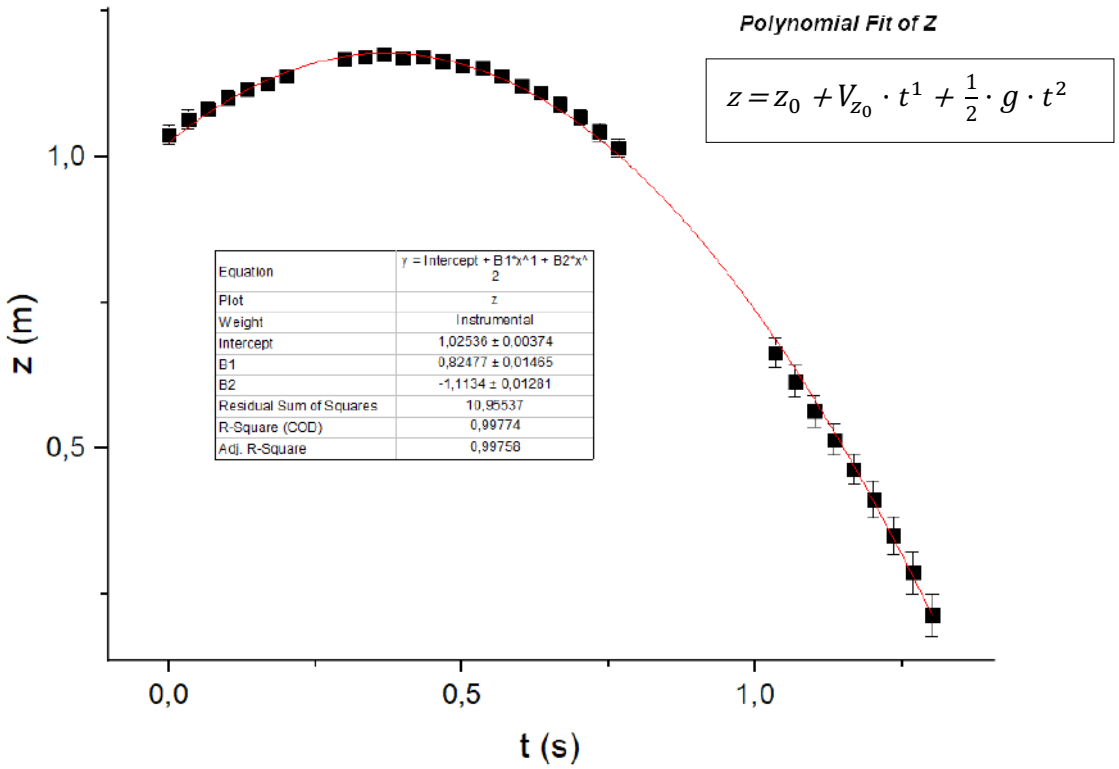

Figure B11 - Comparison between the theoretical model (red) and data collected, considering their maximum error

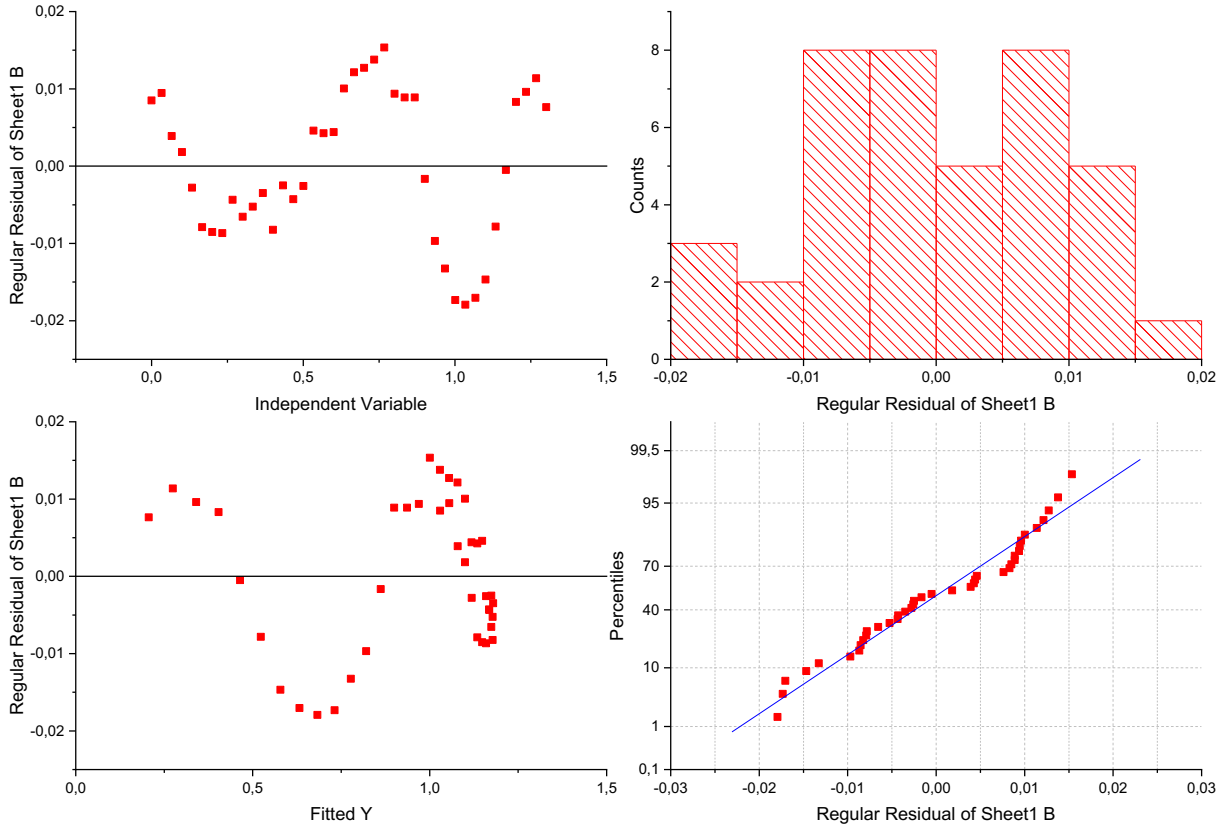

Figure B12 – Origin Pro 2018: study of the variability of the data with respect to the identified equation of motion

The analysis of the variability of the data proposed by the Origin Pro 2018 software in the four diagrams shown in figure B12 highlights some peculiar aspects of the results obtained from the motion tracking. First of all, it should be noted that the distribution of residuals (difference between the observed and estimated values) is relatively disordered, with at least 4 sign changes with respect to the zero axis. Furthermore, the histogram indicates that the random error is normally distributed with the exception of the residual range between +0.01 and +0.02 m, which includes 6 values. Finally, the probability diagram of the residuals based on the percentiles with respect to the ordered residual confirms that the variance is normally distributed since it's approximately linear except for some values at the extremities. All this confirms that the model is significantly validated by the data obtained with the tracing.

B.3.4.2 Other interpretations

A worthwhile factor that we have to take into consideration is the possible flaw in maintaining the correct frame rate with which the scene was shot.

$g'_{av} = \frac{g_{tvm} + g_{or}}{2}$

If $z = z_0 + v_{z0} \cdot t + \frac{1}{2} g_{av} \cdot t^2$ is satisfied, so the equation $z = z_0 + v'_{z0} \cdot t' + \frac{1}{2} g'_{av} \cdot t'^2$ will also be satisfied, where $t' = \frac{t}{\alpha}$; $v'_{z0} = \alpha \cdot v_{z0}$ and $g'_{av} = g_{av} \cdot \alpha^2$ (the quotas in t_x are not modified).

By setting $\alpha = \sqrt{\frac{1{,}62}{2{,}31}} = 0.84$, the same fit can be obtained with the following parameters:

$g = 1.62\ m/s^2$

$v'z0 = 0.992\ m/s \cdot 0.84 = 0.83\ m/s$

$framerate = 29.97\ fps \cdot 0.84 = 25.17\ fps$ *and therefore* $\Delta t = 0.040\ s$

Assuming that the sequence was shot on the Moon, we must therefore assume that the original shooting framerate is 4.8 fps lower than the one that occurred to us as a result of the various video conversions. The sequence we see today would therefore have undergone an acceleration of about 19% compared to the original one: however, this represents a rather problematic result.